**ISTANBUL TECHNICAL UNIVERSITY ★ GRADUATE SCHOOL**

# MICROBIALLY MEDIATED BASALT DISSOLUTION UNDER ACIDIC CONDITIONS

**M.Sc. THESIS**

**Fatih ŞEKERCİ**

**Department of Geological Engineering**

**Geological Engineering Programme**

**JUNE 2021**

**ISTANBUL TECHNICAL UNIVERSITY ★ GRADUATE SCHOOL**

# MICROBIALLY MEDIATED BASALT DISSOLUTION UNDER ACIDIC CONDITIONS

**M.Sc. THESIS**

**Fatih ŞEKERCİ**
**(505181309)**

**Department of Geological Engineering**

**Geological Engineering Programme**

**Thesis Advisor: Prof. Dr. Nurgül BALCI**

**JUNE 2021**

**ISTANBUL TEKNİK ÜNİVERSİTESİ ★ LİSANSÜSTÜ EĞİTİM ENSTİTÜSÜ**

# ASİT KOŞULLAR ALTINDA BAZALTLARIN ÇÖZÜNMESİNDE MİKROBİYAL ETKİLERİN TAYİNİ

**YÜKSEK LİSANS TEZİ**

**Fatih ŞEKERCİ**
**(505181309)**

**Jeoloji Mühendisliği Anabilim Dalı**

**Jeoloji Mühendisliği Programı**

**Tez Danışmanı: Prof. Dr. Nurgül BALCI**

**HAZİRAN 2021**

**Fatih ŞEKERCİ**, an **M.Sc.** student of İTU Graduate School student ID **505181309,** successfully defended the thesis entitled **"MICROBIALLY MEDIATED BASALT DISSOLUTION UNDER ACIDIC CONDITIONS",** which he prepared after fulfilling the requirements specified in the associated legislations, before the jury whose signatures are below.

| | | |
|---|---|---|
| **Thesis Advisor :** | **Prof. Dr. Nurgül BALCI**<br>İstanbul Technical University | ..... |
| **Jury Members :** | **Prof. Dr. Kürşad Kadir ERİŞ**<br>Istanbul Technical University | ..... |
| | **Prof. Dr. Erol SARI**<br>Istanbul University | ..... |

**Date of Submission : 11.06.2021**
**Date of Defense : 28.06.2021**

***To infinity and beyond,***

## FOREWORD

I have always been interested in space since my childhood. Science fiction books and movies were always my favorite ones. Works of Ray Bradbury, Arthur C. Clarke, Frank Herbert, HG Wells, Steven Spielberg elevated my excitement about space and possibility of the extraterrestrial life. I made acquainted with astrobiology and geomicrobiology in the second year of my Bachelor's study at the Molecular Biology and Genetics Department and have followed this path throughout my career. Today, I am writing my M.Sc. thesis about the possibility of using Fe oxides as biosignatures, which may have implications for Martian minerals.

First, I would like to thank my supervisor Prof. Dr. Nurgül Balcı for her support and supervision throughout my M.Sc. journey. She advised and encouraged me to study geology to combine my molecular biology background with geology to have aspects of geomicrobiology, and today I am aware that this was the perfect choice for me. I would like to thank my colleague Yağmur Güneş from Geomicrobiology and Biogeochemistry Laboratory for her help in geology and for motivating me during my study. I also want to thank all members of our laboratory for their comments and help in my study: Ceren Nural, Gamze Özbay, Şevval Yalçınkaya, Doğa Dila Gökgöz, and Hüseyin Sarıkeçe.

I also would like to thank my family for their endless support, love, and trust in me. They always accompanied me in all the situations that I had. I would like to thank my friends for their precious friendship. They always supported me in my decisions, and they always give good advice.

Lastly, I would like to thank Nazlı Dilara Erdoğdu for always being with me.

This M.Sc. thesis was supported by the Research Fund of Istanbul Technical University (Project Number: 42411) and TUBITAK (The Scientific and Technological Research Council of Turkey) grant to Nurgül Balcı (Project Number: 119Y411).

June 2021 Fatih Şekerci

**TABLE OF CONTENTS**

**Page**

## ABBREVIATIONS

**AMD** : Acid mine drainage
**an** : Andesine
**ATCC** : American Type Culture Collection
**aug** : Augite
**BET** : Branauer, Emmett, Teller
**BS1** : Basalt sample 1
**BS1-AB** : Basalt sample 1 – Abiotic
**BS1-B** : Basalt sample 1 – Biotic
**BS2** : Basalt sample 2
**BS2-AB** : Basalt sample 2 – Abiotic
**BS2-B** : Basalt sample 2 – Biotic
**EDS** : Energy dispersive spectroscopy
**g** : gram
**gyp** : Gypsum
**h** : Hour
**jar** : Jarosite
**L** : Liter
**mg** : Miligram
**mL** : Mililiter
**mm** : Milimeter
**mol** : Molarity
**MPN** : Most probable number
**N** : Normality
**NADH** : Nicotinamide adenine dinucleotide (NAD) + hydrogen (H)
**nm** : Nanometer
**NW** : Northwest
**OMEGA** : Observatoire pour la Mineralogie, l'Eau, les Glaces et l'Activité
**rpm** : Revolutions per minute
**rRNA** : Ribosomal RNA

**SEM-EDS** : Scanning electron microscopy with energy dispersive spectroscopy

**tot** : Total

**UV** : Ultraviolet

**XRD** : X-ray powder diffraction

**XRF** : X-ray fluorescence spectrometry

**µm** : Micrometer

## SYMBOLS

| | |
|---|---|
| **&** | : And |
| **ºC** | : Degree celcius |
| **µ** | : Micro |
| **%** | : Percentage |
| ® | : Registered |

**LIST OF TABLES**

**Page**

**LIST OF FIGURES**

**Page**

## MICROBIALLY MEDIATED BASALT DISSOLUTION UNDER ACIDIC CONDITIONS

## SUMMARY

Water-rock-biota interactions are widely distributed processes and regulate elements release and mobility on Earth. By regulating elemental releases, these intimate processes provide macro and micronutrients and thus shape microbial community structure under various environmental conditions. Temperature, salinity, pH, and the concentrations of certain ions in the solution affect rock and mineral weathering. The reactivity of silicate rocks/minerals is highly dependent on the pH of the solution that they are interacting with. The dissolution rate of rock-forming silicate minerals is independent of pH between 5 and 8 but it increases outside of this range, particularly when pH > 8. Silicates may undergo stoichiometric or non-stoichiometric dissolution, the latter is favorable under acidic conditions. Laboratory-based studies demonstrated that the formation of Fe-sulfate, Ca-sulfate, amorphous silica, and iron oxide compounds are among the secondary products of acidic weathering of basalts.

Microbe-rock interactions are common in all three domains of life and have been the subject of intensive research due to their biosignature potential. Chemolithotrophic microorganisms are able to utilize Fe, S, Mn, and other N species in redox reactions to produce energy, that is required for cell synthesis and metabolic reactions thus play an important role in rock weathering.

Acidophilic iron and sulfur-oxidizing chemolithotrophic bacteria *Acidithiobacillus ferrooxidans* was used in the current study to explore the role of the bacteria on the dissolution of two chemically different basalts as well as the biosignature potential of these processes.

For this purpose, two different basalt rocks (BS1 and BS2) crushed and sieved to 0.5-1 mm were used. The Fe-free medium was used as the reactive fluids for the batch experiments. To initiate the experiments, 20 g of basalt grains were added into 200 mL of experimental medium with/without *A. ferrooxidans*. The experimental sets were incubated at 28 $^{o}$C and 130 rpm agitation for 50 days. For each basalt sample, four parallel experiments were set up.

The experimental sets were sampled at days 1, 3, 5, 10, 15, 20, 25, 30, 35, 40, 45, and 50. At each sampling day, 5 mL of aliquots were withdrawn from the experimental container under aseptic conditions and filtered through 0.22 μm syringe filters. $Fe(II)_{aq}$, $Fe_{(tot)}$, $SiO_{2(aq)}$, Ca, and Mg concentrations were measured spectrophotometrically. An additional 2 mL of aliquot was withdrawn from biotic experiments under aseptic conditions and used for an MPN assay to estimate alive bacterial cell number throughout the experiments. The pH values of the solutions were

determined at each sampling day as well. At the end of the each experiment, experimental fluid was filtered and stored at +4 $^{o}$C. Basalt grains and the secondary precipitations in the experimental sets were placed at Petri dishes and air-dried at room temperature, and subsequently kept at -20 $^{o}$C until further analyses. XRD and SEM-EDS analyses were performed on the post-reacted basalt grains to determine possible mineralogical changes and surface chemistry, respectively.

Compared to the initial inoculate of 1.6 x $10^6$ cells/mL, there was an increase in the cell numbers with the extend of the experiments. The maximum bacteria number was determined as 5.4 x $10^8$ cells/mL in BS1-B at day 15, and 2.2 x $10^9$ cells/mL in BS2-B at day 20. Following a decrease in the bacteria number until day 25, the number remained almost constant until the end of the experiment in both sets. An increase in the cell numbers, as well as higher $Fe(III)_{aq}$ in the biotic experiments suggest that the dissolution of basalt grains created a suitable environment for *A. ferrooxidans* for its survival and growth.

The pH values increased with the extent of the reaction and sulfuric acid was added. The reason for the increase in pH was silicate dissolution. Dissolution of silicate minerals consumes dissolved $CO_2$ in water and causes a decline in pH. Additionally, $Fe(III)_{aq}$ undergoes hydrolysis reaction, releasing proton into solution, further contributes to acidity of the solution. The spontaneous oxidation of Fe(II) under acidic conditions is kinetically slow, thus the source of $Fe(III)_{aq}$ was bacterial activity under the current experimental conditions. $Fe(III)_{aq}$ measurements are consistent with biologically catalyzed $Fe(II)_{aq}$ reactions. For example, $Fe_{(tot)}$ and $Fe(II)_{aq}$ concentrations were lower in the biotic experiments than those in the abiotic samples. Identification of Fe-bearing secondary phases in the biotic experiments along with these Fe measurements suggest $Fe(III)_{aq}$ saturated solution chemistry, thus increasing the rate of $Fe(II)_{aq}$ oxidation. This result showed that the most of iron released from basalt grains in biological sets was oxidized by *A. ferrooxidans.* A sharp $SiO_{2(aq)}$ release occurred in the early stage of all experimental sets. A fast decrease in $SiO_{2(aq)}$ concentration occurred in the BS1 samples compared to the BS2 samples. Nonetheless, $SiO_{2(aq)}$ concentrations were nearly similar in all samples at the end of the experiments. Compared to $SiO_{2(aq)}$, Ca released gradually and reached maximum levels between days 25 and 30. Consecutive decrease and increase were measured. Ca release rate was almost similar between biotic and abiotic experiments, slightly higher in the biotic BS2 experiments. Mg release rate was significantly greater in BS2 experiments relative to BS1, as well as biotic experiments. Trivalent cations $Fe^{3+}$ and $Al^{3+}$ have more affinity to react with sulfate ions present in the solution than divalent cations $Ca^{2+}$ and $Mg^{2+}$ under acidic conditions. $Fe(III)_{aq}$ formed by bacterial iron oxidation combine with sulfate leaving Ca and Mg in the solution fluids. The calculated elemental release rates of $SiO_{2(aq)}$, Ca, and Mg were similar between biotic and abiotic experiments but show significant differences among the rock samples, being higher in BS2. Although both basalt samples are mainly composed of andesine and augite, rock crystallinity seems to play a major role during the dissolution reactions.

The fracture structures observed on the post-reacted basalt grains from abiotic experiments were absent in the biotic counterparts but secondary phases as spherical aggregates with a size of 1 μm or smaller were only present on the surface of biotically reacted rock grains. EDS spectra of these phases showed Fe and S and K enrichment and XRD analysis revealed the secondary precipitation is primarily composed of

jarosite and gypsum. The formation of these two minerals was only measurably detected in the biotic experiments, raising the possibility of using the respected minerals as biosignature on Earth and Mars but more detailed mineralogical and morphological studies should be undertaken.

# ASİT KOŞULLAR ALTINDA BAZALTLARIN ÇÖZÜNMESİNDE MİKROBİYAL ETKİLERİN TAYİNİ

## ÖZET


Su-kayaç-mikroorganizma etkileşimleri doğada yaygın bir şekilde bulunan süreçlerdir ve bunun sonucunda canlıların metabolizmaları için gerekli olan elementlerin ortama salınımını ve Yerküre'deki döngülere katılmasını sağlarlar. Kayaçlardan ortama salınan elementler mikroorganizmalar tarafından makro ve mikro besinler olarak kullanılabilirler ve bundan dolayı bu etkileşimler farklı çevresel ve jeokimyasal koşullardaki mikrobiyal komünitenin şekillenmesine neden olurlar. Sıcaklık, tuzluluk, pH ve belirli iyonların solüsyon içerisindeki konsantrasyonu kayaç ve mineral ayrışmalarını etkilerler. Silikat minerallerinin ayrışmaları etkileşimde bulundukları solüsyonun pH değerinden önemli oranda etkilenmektedir. Kayaç yapıcı silikat minerallerinin ayrışma oranları 5 ve 8 arasındaki pH değerlerinde önemli bir değişiklik göstermezken pH değeri bu aralığın dışına çıktıkça artmaktadır. Silikatlar stokiyometriye uygun veya aykırı bir şekilde ayrışabilmektedirler. Asidik koşullar altında ise genellikle stokiyometriye aykırı bir çözünme gerçekleşmektedir. Laboratuvar temelli çalışmalar bazaltların asidik ayrışmaya uğramaları sonucunda demir sülfat, kalsiyum sülfat, amorf silika ve demir oksit bileşiklerinin oluştuğunu göstermiştir.

Mikroorganizma-kayaç etkileşimleri yaşamın üç alanına ait canlılarda yaygın bir şekilde gerçekleşmektedir ve biyoiz potansiyellerinden dolayı birçok araştırmaya konu olmuşlardır. Kemolitotrofik organizmalar demir, kükürt, manganez ve diğer azot bileşiklerini redoks reaksiyonlarına sokarak metabolizmaları için gerekli olan enerjiyi üretmektedirler ve kayaç ayrışmasında önemli bir rol oynamaktadırlar.

Bu çalışmada asidofil demir ve kükürt oksitleyici kemolitotrofik bakteri *Acidithiobacillus ferrooxidans*'ın iki farklı bazalt kayacının çözünmelerinde oynadığı rol ve bu etkileşimin biyoiz potansiyeli araştırıldı. Bu amaçla iki farklı bazalt kayacı (BS1 ve BS2) öğütüldü ve 0.5-1 mm boyutundakiler eleme yoluyla seçilerek hazırlandı. Deney setleri hazırlanırken *A. ferrooxidans*'ın bazalttan gelen demiri kullanması için demir içermeyen solüsyon kullanıldı. 20 g bazalt 200 mL deney solüsyonu içerisine eklenerek abiyotik deney setleri ve aynı koşullara *A. ferrooxidans* eklemesiyle biyotik deney setleri hazırlandı. Hazırlanan setler 50 gün boyunca 28 ºC sıcaklıkta 130 rpm'de çalkalanmaya maruz bırakıldı. Her bazalt örneği için dört paralel deney seti hazırlandı.

Deney setleri 1, 3, 5, 10, 15, 20, 25, 30, 35, 40, 45 ve 50. günlerde örneklendi. Her örneklemede 5 mL'lik alikot steril koşullar altında alındı ve 0.22 µm şırınga filtreleri kullanılarak filtrelendi. Solüsyon içerisindeki Fe(II), $Fe_{(tot)}$, $SiO_{2(aq)}$, Ca ve Mg konsantrasyonları spektrofotometrik olarak ölçüldü. Ayrıca yine steril koşullar altında

biyotik deney setlerinden 2 mL daha örnekleme yapıldı ve canlı bakteri sayısının takip edilmesi amacıyla MPN analizinde kullanıldı. Ayrıca deney solüsyonlarının her örneklemede pH değerleri takip edildi. Deney sonunda deney solüsyonu filtrelendi ve +4 $^{o}$C'de saklandı. Bazalt taneleri ve deney setlerinde oluşan ikincil çökeltiler Petri kaplarına koyularak oda koşulları altında kurutuldu ve sonrasında yapılacak analizler için -20 $^{o}$C'de saklandı. Deney sonlarında elde edilen reaktif bazaltların mineralojik ve yüzey kimyasında meydana gelecek olası değişimlerin incelenmesi için XRD ve SEM-EDS analizleri yapıldı.

Deney setlerinde kullanılan bakteri sayısı deney öncesinde 1.6 x $10^6$ hücre/mL olarak belirlendi. Maksimum bakteri sayısı BS1-B setinde 15. günde 5.4 x $10^8$ hücre/mL, BS2-B setinde 20. günde 2.2 x $10^9$ hücre/mL olarak saptandı. Bakteri sayısında 25. günde gözlemlenen düşüşün ardından deney sonuna kadar değerler önemli bir değişim göstermedi. Biyotik deney setlerinde bakteri sayısı ve $Fe(III)_{aq}$ konsantrasyonu arasındaki paralel artış bazalt çözünmesinin *A. ferrooxidans*'ın hayatta kalması ve çoğalması için uygun bir ortam sağladığını gösterdi.

Tüm deney setlerinde solüsyonların pH değerlerinde silika çözünmesine bağlı olarak artışlar belirlenmiştir. Silikat minerallerinin çözünmesi sudaki çözünmüş $CO_2$'i tüketmektedir ve bunun sonucu olarak pH değerinde artışa sebep olmaktadır. Bu reaksiyonlar sonucu pH yükselmektedir. Ayrıca sudaki $Fe(III)_{aq}$ hidroliz reaksiyonuna girerek solüsyona proton salınmasına sebep olmakta ve solüsyonun asitliğinin devam etmesini sağlamaktadır. Fe(II)'nin asit koşullar altında kimyasal olarak oksitlenme kinetiği oldukça düşüktür, bundan dolayı deney setlerindeki $Fe(III)_{aq}$ artışının sebebi bakteriyel aktivitedir. Abiyotik deneylere oranla biyotik deneylerde ölçülen $Fe(III)_{aq}$ konsantrasyonları bakteriyel aktiviteleri desteklemektedir. Solüsyondaki $Fe_{(tot)}$ ve Fe(II) konsantrasyonları biyotik deney setlerindeki abiyotik karşılıklarından daha düşük ölçüldü. Biyotik deney setlerindeki demir içeren ikincil oluşumlar solüsyonun kimyasal olarak demirce doygunlaştığını ve Fe(II)'nin oksidasyon oranının arttığını göstermektedir. Bu sonuçlar biyolojik deney setlerindeki bazalt tanelerinden salınan $Fe(II)_{aq}$'nin çoğunluğunun *A. ferrooxidans* tarafından oksitlendiğini göstermiştir. Tüm deney setlerinde başlangıçta hızlı bir $SiO_{2(aq)}$ salınımı gerçekleşti. Sonrasında BS1 setlerinde BS2 setlerine göre daha hızlı bir $SiO_{2(aq)}$ düşüşü gözlemlendi. Buna rağmen deney sonunda tüm deney setlerindeki $SiO_{2(aq)}$ konsantrasyonu benzer seviyede belirlendi. $SiO_{2(aq)}$ ile karşılaştırıldığında Ca konsantrasyonu daha kademeli olarak artış gösterdi ve 25 ila 30. günler arasında setlerde maksimum değere ulaştı. Sonrasında birbirini takip eden azalış ve artışlar belirlendi. Biyotik ve abiyotik deney setlerinde Ca salınımı benzer değerlerde belirlendi, BS2-B setinde ise diğer setlere nazaran biraz daha yüksek Ca değerleri ölçülmüştür. Mg salınım oranları BS2 setlerinde BS1 setlerine göre ve biyotik setlerde abiyotiklere göre önemli oranda daha yüksek belirlendi. Asidik koşullar altında üç değerliğe sahip katyonlar $Fe^{3+}$ ve $Al^{3+}$, iki değerlikli katyonlar $Ca^{2+}$ ve $Mg^{2+}$'a göre solüsyon içerisinde bulunan sülfat iyonları ile daha fazla etkileşime girme eğilimine sahiptir. Bakteriyel oksidasyon sonucu oluşan $Fe(III)_{aq}$ solüsyondaki sülfat iyonları ile birleşirken kalsiyum ve magnezyumun sıvı içerisinde kalmasına sebep oldu. Hesaplanan $SiO_{2(aq)}$, Ca ve Mg değerleri biyotik ve abiyotik deney setlerinde benzerken, BS2 kayacında BS1 kayacına göre daha yüksek belirlendi. İki kayaç da çoğunlukla andezin ve ojit minerallerinden meydana gelse de kayaç kristalinitesinin ayrışma reaksiyonlarında önemli bir etken olduğunu göstermektedir.

Ayrışma sonrasında SEM analizlerinde abiyotik deney setlerindeki bazalt tanelerinde çatlaklı yapılar gözlemlenirken bunlar biyotik ayrışmaya uğrayan tanelerde gözlemlenmemiştir. Bunun yerine biyotik deney setlerinden alınan bazalt tanelerinin üzerinde 1 μm ve daha küçük boyutlarda yuvarlak ikinci oluşumlar gözlemlendi. EDS analizleri bu çökeltilerin demir, kükürt ve potasyumca zenginleşme olduğunu gösterirken XRD analizleri yalnızca biyotik deneylerin sonunda elde edilen sarı çökeltinin demir sülfat minerali jarosit ve kalsiyum sülfat minerali olan jips olduğunu ortaya koydu. Bu iki mineralin sadece biyotik deney setlerinde tespit edilmesi bunların Yerküre ve Mars'taki benzer koşullar için bir biyoiz potansiyeli taşıyabileceğini önermektedir. Ancak, daha detaylı ve kontrollü deneyler ile bu oluşumlara ait ayrıntılı mineralojik ve morfolojik çalışmaların yürütülmesi gerekmektedir.

# 1. INTRODUCTION

## 1.1 Basalt Weathering under Acidic Conditions

Chemical weathering of rocks and minerals during the interactions between water and biota is one of the key processes that continuously influence elemental release throughout the Earth's history (Schwartzman & Volk, 1989). By regulating elements release, water-rock interactions profoundly influence and shape biodiversity by providing necessary nutrients and bioessential elements. Additionally, dissolution of rocks and minerals, in particular silicates, and subsequent formation of the secondary phases have significantly contributed to Earth's climate by consuming $CO_2$. This $CO_2$ consumption affects the global temperature by the drawdown of atmospheric $CO_2$, which is one of the greenhouse gases in Earth's atmosphere (Cockell et al., 2016). It was argued that the chemical weathering of basaltic rocks is responsible for 30-35% of the atmospheric $CO_2$ breakdown (Dessert et al., 2003).

The chemistry of reactive fluids that the rocks interact with and environmental factors such as temperature, salinity, pH, and the concentration of certain cations and anions are the parameters that change dissolution kinetics and rates of minerals and rocks. Among them, the pH of the solution influences the reactivity of both solvent and geological material. Silicate dissolution is pH-independent between 5 and 8, but the dissolution rate of silicate minerals increases as the acidity or alkalinity increases excluding this range (Welch & Ullman, 1993; Gudbrandsson et al., 2011).

Acidic dissolution rate and kinetic of silicate rocks, in particular Fe-bearing ones, have been the subject of intensive research mainly due to the presence of diverse microbial community harboring these types of rocks as well as influence of Fe(II) oxidizing microorganisms to Fe cycles at basaltic rock terrain. In addition, identification of basaltic rocks on Mars surface along with the presence of Fe oxides fuel the interest to test if some of these Fe-oxides may in fact carry putative life traces (Fairén et al., 2010).

Two different dissolution mechanisms are widely accepted for silicate rocks /minerals: Congruent (stoichiometric) dissolution and incongruent (nonstoichiometric) dissolution. Congruent, or stoichiometric dissolution refer to rock dissolution when the molar ratios of the elements in the solution, which are released from the mineral/rock, are the same as the molar ratios in the mineral formula, while the nonstoichiometric dissolution refers otherwise, thus different molar ratios (Brantley, 2008). The dissolution-reprecipitation mechanism is argued for the stoichiometric dissolution of a mineral, and following precipitation of secondary phases. On the other hand, leaching is the proposed mechanism for nonstoichiometric dissolution due to the differences in site energies of cations in the mineral structure (Brantley, 2008). Under acidic conditions, nonstoichiometric dissolution is generally proposed for silicate dissolutions. Leaching causes monovalent metal-oxide bonds to break faster than divalent and trivalent metal-oxide bonds while Si-O bonds break last (Schott et al. 2009). However, Hellmann et al. (2012) stated that the dissolution-reprecipitation mechanism is valid for all mineral dissolution, but the formation of secondary silicate-rich phases causes the difference in the molar ratios of dissolved elements in solution. Hence, element release rates may provide insights into the dissolution mechanisms of silicate minerals/rocks.

Tosca et al. (2004) incubated basalt, basaltic andesine, and glass samples with similar composition under acidic fluids with a pH range of 0-4, for 14 days. In the case of crystalline rocks, sulfate minerals and amorphous silica precipitations were detected under highly acidic conditions, and iron oxide formations were observed under moderately acidic conditions. Amorphous silica and Fe/Mg sulfates were precipitated during olivine dissolution, and Ca-sulfate minerals formed by the dissolution of Ca-bearing plagioclase, feldspar, and pyroxene minerals in both basalt and basaltic andesine. In a later study, Hurowitz et al. (2005) prepared a flow-through system with basalts continuously replenished by acidic fresh fluid, and batch experiments with water:rock ratio 100 and 1000 for 17 days. Sulfate and amorphous silica formations were identified in all the experiments, but sulfate formation was higher in batch experiments. In addition, SEM and Raman analyses detected a minor amount of the poorly crystalline iron oxide phases. In a recent study, McCollom et al. (2013) submerged basalt phenocrysts in 1.0 M sulfuric acid at 145 $^{o}$C at different fluid:rock ratios ranging from 1.1 to 10.3 Major products of the respective experimental system

contained amorphous silica, Fe-rich natroalunite, limited formations of iron oxides/hydroxyoxides phases with other sulfates.

### 1.2 Microbial Weathering of Basalts

Biological weathering is a widespread process in nature and caused by the organisms in all three domains of life: Bacteria, Archaea, and Eukarya (Uroz et al., 2009). Chemolithotrophic microorganisms can reach the cations such as sulfur, iron, manganese, and nitrogen species that are released from geological materials, and produce the energy required for their essential metabolism via oxidation-reduction reactions, thus they play a significant role in the rock weathering (Norlund et al., 2009; Bauermeister et al., 2013; Navarrete et al., 2013; Kuypers et al., 2018; Daye et al., 2019; Napieralski et al., 2019). Biological weathering is not restricted to surface microbial communities, it is also a widely distributed metabolic process in subsurface conditions. 16S rRNA analyses showed the existence of chemolithoautotrophic microorganisms in deep subsurface environments (Teske, 2005). This great diversity in microbial species and metabolic flexibility has significant consequences in terms of weathering of rocks and minerals. For example, some of the microorganisms may increase the weathering rate while others cause an inhibition (Barker et al., 1997). Increasing the acidity of the solution by organic acid production (Drever & Stillings, 1997), creating a microenvironment and changing the water chemistry between rock surface and microbial cells by forming biofilm (Brehm et al., 2005), and using siderophores and other chelating molecules to increase ligand binding activity (Welch & Ullman, 1996; Perez et al., 2016) are some of the microbial mechanisms that cause the acceleration weathering rate of rocks and minerals. On the other hand, microbially catalyzed secondary mineral formation and precipitation (e.g ferric ion complexes) on the surface of mineral acting as a barrier between a mineral and reactive fluid are one of the inverse effects of microbial metabolisms resulting in a decrease in weathering rate of rocks/minerals (Santelli et al., 2001; Welch & Banfield, 2002; Garcia et al., 2013). By providing bioessential elements such as Ca, Mg, Fe silicate weathering plays a significant role in shaping the biosphere and likely create macro/microenvironments with plausible biosignature potential. Biogenic tubular structures (Banerjee et al., 2011; Knowles et al., 2013), organic matter preservation along with secondary phase minerals (Preston et al., 2011; Türke et al., 2018), microfossils (McKinley et al., 2000) as well as variations in element release rates and thus concentration of certain elements

(e.g., Ca, Mg) can be considered as biosignatures. Specific elemental release and enrichment rates are proposed as potential biosignatures in basalt and basaltic glasses (Léveillé et al., 2007; Hausrath et al., 2009). Therefore, understanding microbial influences on weathering of silicates and their subsequent possible secondary products may help us to develop the ability to distinguish a feature of chemically produced reaction products from those that can solely be attributed to biological reactions.

There are various laboratory-based studies about the microbial weathering of basalt and basaltic glass in different conditions and with diverse microbial organisms. Wu et al. (2007) prepared experimental sets including 45-850 μm-sized basalt samples with heterotrophic bacteria *Burkholderia fungorum* in P-limited medium with the pH range of 4.34-6.88 at 28 $^{o}$C for 36 days. The pH decrease in the experimental samples by $CO_2$ production with aerobic respiration and organic acid release from bacteria increased the release rates of Ca, Mg, Si, and Sr. P-limited medium cause the bacteria to elevate the dissolution of P-bearing mineral apatite in basalt. Olsson-Francis et al. (2017) carried out a similar experiment with *Burkholderia* sp. strain B_33 with basalt grains (0.5-1 mm) in minimal bacterial growth medium with pH 7.0 for 28 days at 25 $^{o}$C. Bacterial activity in the system resulted in the formation of iron-hydroxide phases and kaolinite while the abiotic system did not cause such formations. Olsson-Francis et al. (2012) incubated cyanobacteria *A. cylinrica, S. elongatus, Leptolyngbya* strain OU_13, *Phormidium* strain OU_10, *Chroococcidiopsis* 029, and *Gleocapsa* strain OU_20 with basalt and rhyolite rocks in 10 mM $NaNO_2$ solution for 45 days with an initial pH value 6.6 at 25 $^{o}$C. Cyanobacterial growth in the experimental sets caused a rise in the pH value via photosynthesis and accelerated the basalt dissolution causing an increase in the release rates of Ca, Mg, Si and K. Navarrete et al. (2013) conducted basalt powder (<0.71 mm) with iron-oxidizing bacteria *A. ferrooxidans* with starting pH 2.4. *A. ferrooxidans* bacteria could grow for 50 days by deriving Fe from basalt. In addition, *A. ferrooxidans* caused to increase in leaching of Fe, Al, and Ti, but not silica from basalt powders. Gunes and Balci (2021) carried out an experiment with halophilic heterotrophic microorganism *Virgibacillus marismortui* with powder-sized (<63 μm) basalt and basaltic andesine at neutral pH. The acidity caused by glucose consumption of bacteria changed the solution chemistry and resulted in an acceleration on silicate dissolution.

This thesis aims to constraining the role of Fe(II) oxidizing bacteria *Acidithiobacillus ferrooxidans* on the dissolution of two basaltic rocks with different Fe compositions under acidic conditions and further exploring possible inorganic biosignatures (i.e. secondary phases, elemental release rates) that can be applicable to acidic conditions.

### *1.3 Acidithiobacillus ferrooxidans*

*Acidithiobacillus ferrooxidans* (formerly: *Thiobacillus ferrooxidans*) is an acidophilic iron- and sulfur-oxidizing chemolithotrophic bacterium that has 30 $^{o}$C and pH 2 optimum growth conditions (Valdés et al., 2008). It is generally found in natural acidic iron- and sulfur-rich environments that are formed by oxidation of sulfide minerals known as acidic mine drainage (AMD) sites (González-Toril et al., 2003). Microbial ecology analyses of various AMD sites revealed the existence of *A. ferrooxidans* (Schrenk et al., 1998; Baker & Banfield, 2003; González-Toril et al., 2003; Aytar et al., 2015; Méndez-García et al., 2015; Huang et al., 2016; ; Sağlam et al., 2016).

The main metabolic activity of *A. ferrooxidans* is the oxidation of Fe(II) to Fe(III) by using low pH of the acidic water to generate opposite electron flow from $Fe^{2+}$ to NADH (Valdés et al., 2008). *A. ferrooxidans* has the ability to oxidize various sulfur compounds such as pyrite elemental sulfur, and other reduced sulfur compounds (Balci et al., 2007, 2012; 2017; Zhan et al., 2019). Under anaerobic conditions, *A. ferrooxidans* can also reduce Fe(III) to Fe(II) (Sand, 1989). Genome sequence studies showed that *A. ferrooxidans* has genes that are related to $CO_2$ fixation via Calvin reductive pentose phosphate cycle and nitrogen fixation (Gale & Beck, 1967; Mackintosh, 1978; Valdés et al., 2003; Valdés et al., 2008). Because structural stabilities of organic matters are low under acidic conditions, *A. ferrooxidans* may play a primary producer role for heterotrophic acidophilic microorganisms in the nutrient-limited AMD sites.

*A. ferrooxidans* was used in various silicate dissolution experiments. For example, Santelli et al. (2001) prepared a batch experiment with Fe-silicate mineral fayalite and *A. ferrooxidans* at initial pH values 2, 3, and 4. It was demonstrated that fayalite dissolution could create a suitable environment for bacterial growth. On the other hand, the bacterial activity resulted in a decrease in fayalite dissolution due to Fe(III) production and subsequent Fe precipitation by the bacteria. Welch and Banfield (2002) investigated the effect of *A. ferrooxidans* on fayalite surface morphology during the

bacterial weathering at an initial pH of 2.0. Transmission electron microscopy (TEM) results of the study demonstrated that the laihunite ($Fe(II)Fe(III)_2(SiO_4)_2$)like layer formation on the fayalite surface as a result of bacterial metabolism created a barrier between mineral and the reactive fluid diminishing the fayalite dissolution. Consistent with Welch and Banfield (2002). Dopson et al. (2009) reported a decrease in augite, biotite, hornblende, microcline, and olivine dissolution rate conducted with *A. ferrooxidans* at pH 2.0. The authors attributed the decrease in dissolution rate to microbially induced of a secondary mineral formation such as jarosite and gypsum acting as a barrier between mineral and the reactive fluid.

## 2. MATERIALS AND METHODS

### 2.1 Rock Sample Preparation

Two different basalt rock samples were prepared and used for the experiments carried out during this study. Major oxide contents of the rock samples were analyzed with X-ray Fluorescence Spectrometry (XRF) and provided in Table 2.1., and mineralogical compositions were detected with X-ray Diffraction Spectrometry (XRD) and provided in Figure 2.1.

**Table 2.1:** Major oxide compositions of BS1 (Basalt sample 1) and BS2 (Basalt sample 2) in weight percent (wt%).

| Major Oxide | BS1 | BS2 |
|---|---|---|
| $SiO_2$ | 46,07 | 48,6 |
| $Al_2O_3$ | 13,21 | 15,9 |
| $Fe_2O_3$ | 12,04 | 9,01 |
| CaO | 10,91 | 8,76 |
| MgO | 9,25 | 9,44 |
| $Na_2O$ | 3,14 | 3,61 |
| $K_2O$ | 1,51 | 1,97 |
| $Cr_2O_3$ | 0 | 0,07 |
| $TiO_2$ | 2,83 | 1,46 |
| MnO | 0,16 | 0,14 |
| $P_2O_5$ | 0,76 | 0,51 |
| SrO | - | 0,08 |
| BaO | - | 0,07 |
| LOI | 2,83 | 1,62 |
| Total | 99,88 | 101,24 |

Altered parts of the rock samples were carefully removed before used in the experiments, and only unaltered, fresh parts of the rock samples were prepared for the experiments. The rock samples were crushed and grounded in a jaw crusher and sieved to 0.5 and 1 mm particle size by using proper sieves. Subsequently, the basaltic grains were sonicated to clean surface bounded fine particles. During ultrasonication, the rock grains were sonicated with distilled water, and this process was repeated until the distilled water gained a clean look. Subsequently, basaltic grains were washed three times with acetone to sterilize their surfaces and kept overnight at room temperature

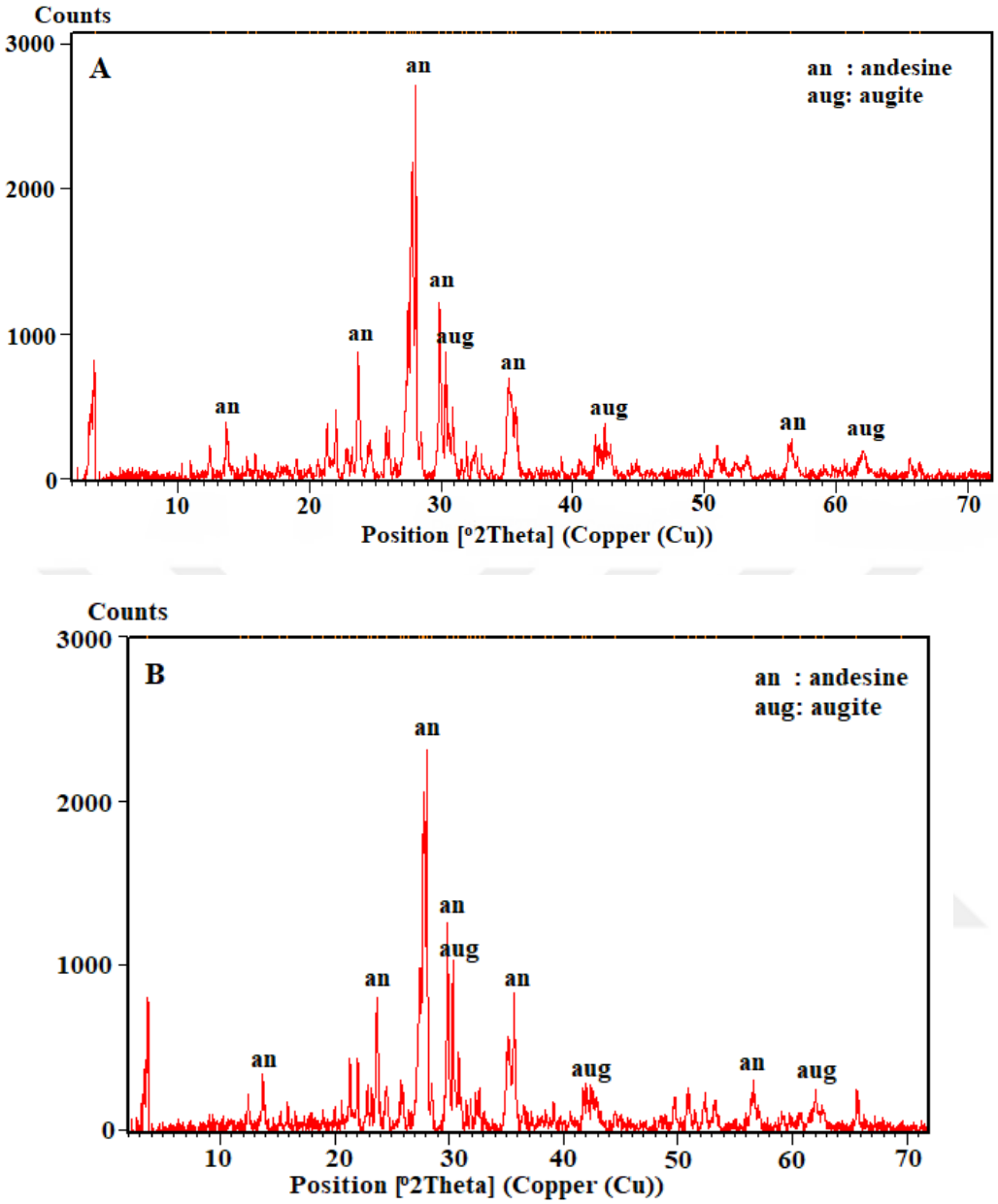


**Figure 2.1:** Mineralogical compositions of (a) BS1 and (b) BS2 rock samples before experiments.

for air-drying before used in the experiments. The surface area of the rock grains was determined by BET (Branauer, Emmett, and Teller) analysis with $N_2$ (10 h degassing time at 50 $^oC$) as 8.17 $m^2/g$ and 7.71 $m^2/g$ for BS1 and BS2 rock samples, respectively at Middle East Technical University.

## 2.2 Model Microorganism, Media, and Growth Conditions

*Acidithiobacillus ferrooxidans* type strain (ATCC 23270) was used for this thesis. The pure culture of *A. ferrooxidans* was obtained from American Type Culture Collection (ATCC) and was maintained in an optimum media.

The actively growing culture of *A. ferrooxidans* was obtained by cultivation in the growth medium (Table 2). The growth medium was prepared by mixing three different solutions. The basal solution was prepared by dissolving below salts in 950 mL of ultrapure water (Human-18 MΩ $cm^{-}1$) and subsequently pH of the basal solution was adjusted to pH 2.0± 0.2 with trace metal grade 10 N $H_2SO_4$ (Merck) 1 mL of the trace elements solution prepared by using the following trace elements was added to the basal solution and the mixture was autoclaved at 121 $^oC$ for 20 minutes. The iron (II) solution was prepared by dissolving Fe(II) sulfate in ultrapure water acidifed to pH=1.2 to prevent Fe(II) oxidation. Fe(II) solution was sterilized by using a sterile 0.22 μm syringe filter. Finally, the sterile Fe(II) solution was added to the basal growth medium in a laminar flow. Then, *A. ferrooxidans* bacteria were incubated with the prepared growth medium at 28 $^oC$ at 130 rpm for 15 days. *A. ferrooxidans* was three times sub-cultured in the medium before the rock experiments (Figure 2.2).

**Table 2.2:** Composition of the *A. ferrooxidans* growth medium.

| Solution | Ingredient | Amount |
|---|---|---|
| Basal solution | $(NH_4)_2SO_4$ | 1 g |
| | $K_2HPO_4$ | 0.4 g |
| | $MgSO_4.7H_2O$ | 4 g |
| | Ultra-pure water | Up to 950.0 mL |
| | pH | 2.0 |
| Iron solution | $FeSO_4.7H_2O$ | 33.3 g |
| | 0.25 N $H_2SO_4$ | Up to 50.0 mL |
| | pH | 1.2 |
| Trace elements solution | $CuSO_4.5H_2O$ | 0.05 mg |
| | $H_3BO_3$ | 0.20 mg |
| | $MnSO_4.H_2O$ | 0.20 mg |
| | $Na_2MoO_4.2H_2O$ | 0.08 mg |
| | $CoCl_2.6H_2O$ | 0.06 mg |
| | $NiCl_2.6H_2O$ | 0.01 mg |
| | $ZnSO_4.7H_2O$ | 0.09 mg |
| | Ultra-pure water | 1000.0 mL |

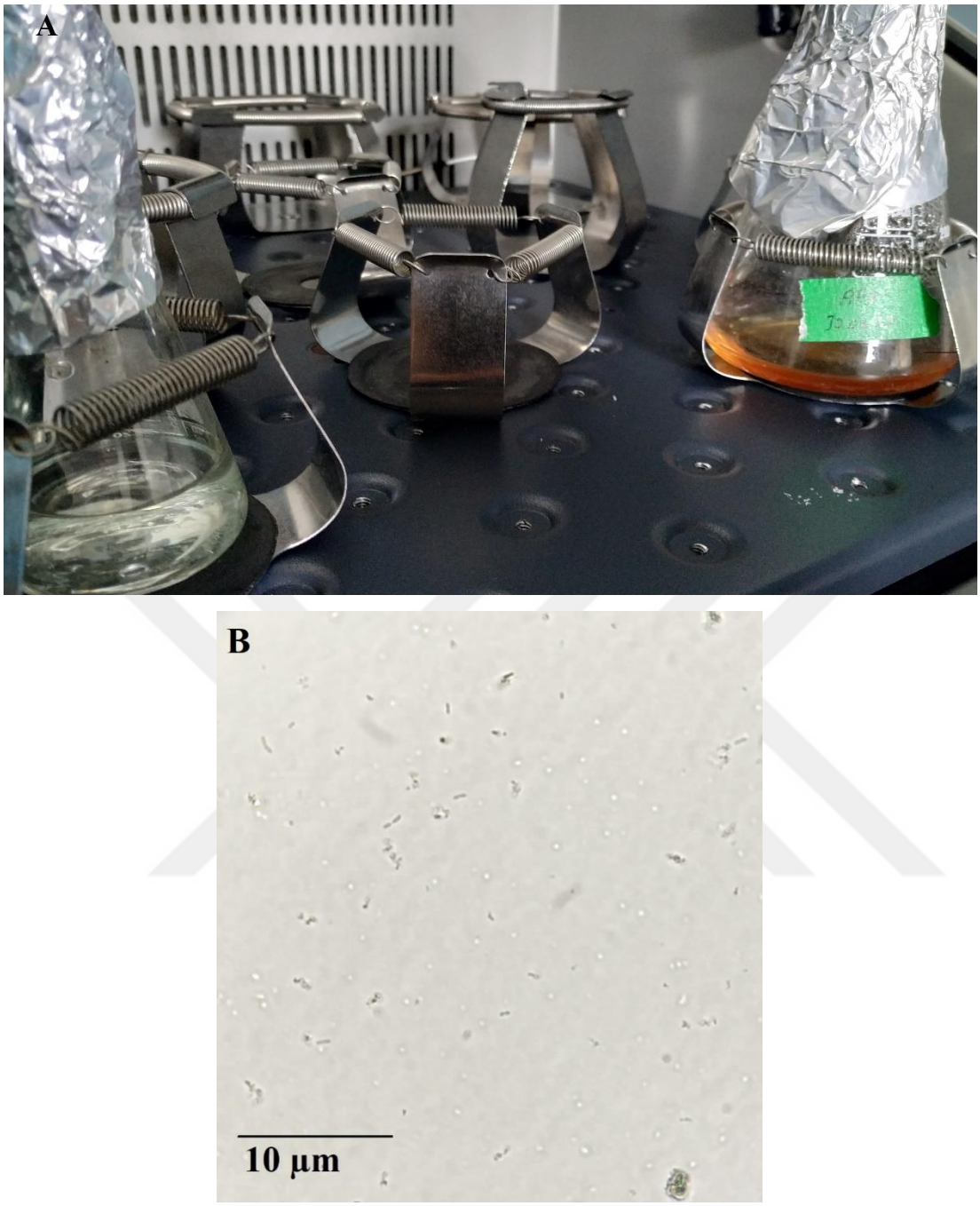


**Figure 2.2:** (A) *A. ferrooxidans* culture. Growth medium without bacteria (Control group), right: Growth medium with *A. ferrooxidans*, red color indicates bacterial iron oxidation. (B) Actively growing *A. ferrooxidans* culture (polarizan microscope).

### 2.3 Experimental Setup

All rock dissolution experiments were performed in batch flasks (Figure 2.3). Prior to use in all of the experiments, the rock samples, previously ground and cleaned, were sterilized. For sterilization, the rock samples were soaked with 70 % ethanol and

spread in a thin layer under UV radiation (germicidal) in a sterile hood for~30 minutes to decontaminate the surface. These sterilization methods were effective since contamination was not observed in the abiotic control experiments. Following these treatments, the rock samples were immediately placed in sterile experimental containers, which were previously acid washed with ultrapure 10 mM $HNO_3$ (Merck).


**Figure 2.3**: The experimental flasks contain basalt particles.

A Fe(II) free medium prepared in the same ways as the growth medium was used in all rock experiments. In order to prepare cell cultures for the biological incubation experiments, actively growing *Acidithiobacillus ferrooxidans* culture was centrifuged at 10.000 rpm for 10 minutes at 4 $^{o}$C to collect the cells. The obtained cell pellet was rinsed several times with the experimental medium to remove possible iron phases that were present in the growth medium. The bacterial cell numbers were calculated with the MPN method (Most probable number assay) as 1.6 x $10^6$ cells/mL by the time experiments were set up.

Four different experimental sets were conducted for each basalt sample: For BS1 basalt sample abiotic (BS1-AB) and biotic (BS1-B) and BS2 basalt sample abiotic (BS2-AB), and biotic (BS2-B) along with each replicate. 20 g of the sterilized basalt grains and 200 mL of experimental medium were placed in 500 mL flasks with and without *A. ferrooxidans* bacteria. These flasks were agitated at 130 rpm at 28 $^{o}$C for 50 days.

pH of the experiments was initially adjusted to 2.0 with ultrapure HCI, and continuously monitored to keep pH under 3.0, and acid was added into the experimental solution when it was necessary. All experiments were conducted in duplicates. Abiotic experiments were conducted under exactly similar conditions to each biotic experiment.

Incubated experimental flasks were sampled on days 1, 3, 5, 10, 15, 20, 25, 30, 35, 40, 45, 50, and at the end of the experiments (Figure 2.4). At each time interval 5 mL of aliquot was aseptically withdrawn from the flasks to measure pH, $Fe(II)_{aq}$, $Fe_{tot}$, $SiO_{2(aq)}$, Ca, and Mg concentrations. An additional 2 mL was used for the MPN method to estimate the number of alive *A. ferrooxidans* in the biological sets. At the end of each experiment, the remaining experimental fluids carefully removed from the flasks were centrifuged at 10.000 rpm and 4 $^{o}$C for 10 minutes to collect possible secondary phases and subsequently, the supernatant was filtered by using 0.22 µm sterile syringe filters (Merck) and stored at +4 $^{o}$C for further analyses. The collected secondary phases and the reacted basaltic grains were placed in Petri dishes and air-dried at room temperature (Figure 2.5). Following the drying step, these samples were stored at -20 $^{o}$C until further microscopic analysis.

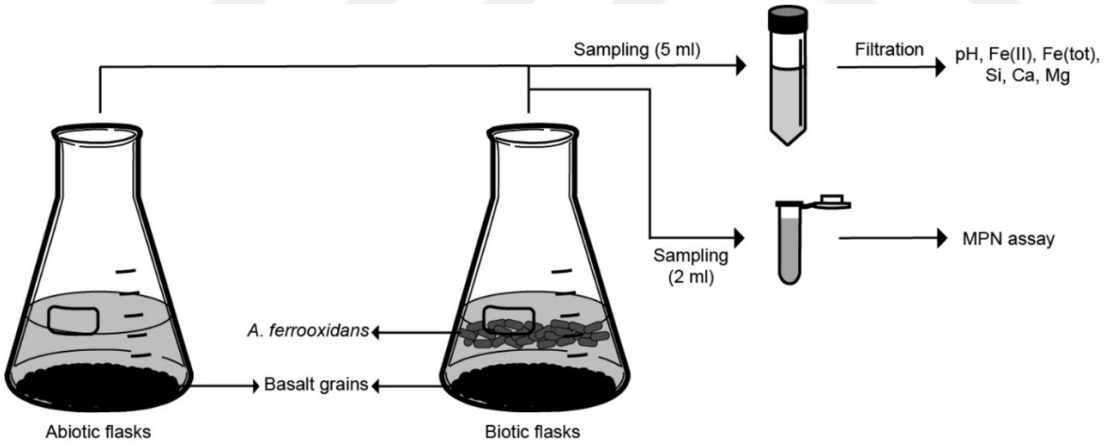


**Figure 2.4:** A schematic representation of experimental setup and sampling process.

## 2.4 Monitoring Bacterial Growth

The most probable number (MPN) assay was used to estimate the viable bacterial cell numbers during the course of the experiments. MPN technique is a statistical widely used method for quantitative estimation of bacterial numbers in water samples. The method is based on making serial dilutions of the bacterial sample and incubating prepared solutions to observe the visual color difference. Color or turbidity changes in

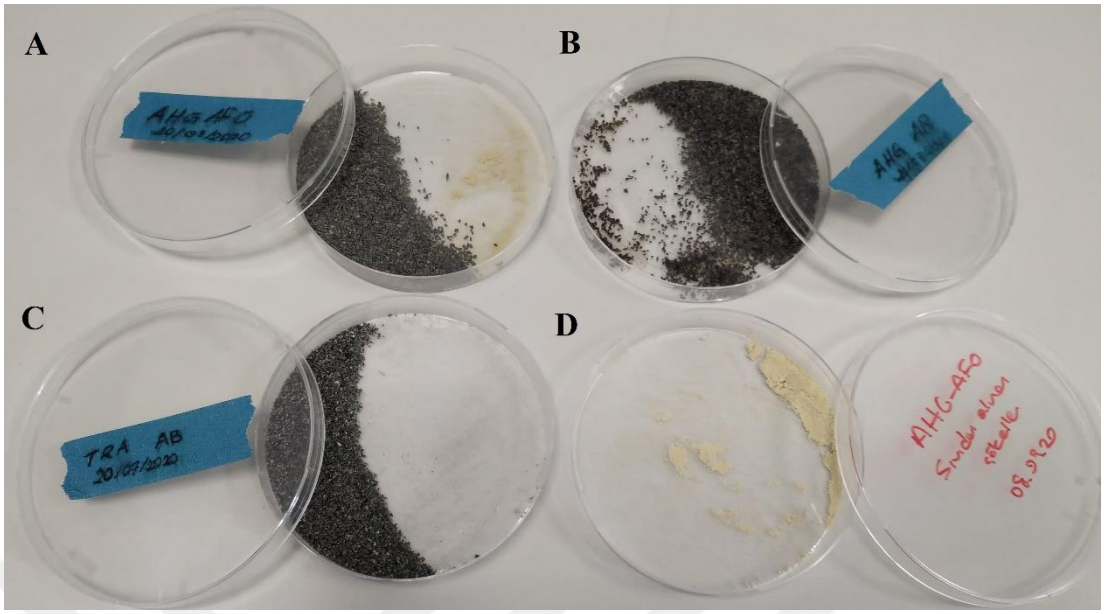


**Figure 2.5:** Air-dried post reacted (A-C) rock grains and (D) the secondary precipitates.

the wells are correlated with an MPN table. MPN index number is based on the statistical probability of the most probable number of bacteria in the original sample. The MPN table that was used in this study has MPN index numbers with 95% confidence level. For MPN estimation 2 mL of aliquot was obtained from each biological set and was inoculated into the growth medium of *A. ferrooxidans* by using serial dilution techniques. Five replicates for each dilution were performed in a 96-well plate and incubated for 14 days by observing visual color changes as an indication of bacterial Fe(II) oxidation (Figure 3.2). The qualitative color-based results were later compared to the MPN table (Appendix A) to estimate the viable *Acidithiobacillus ferrooxidans* number via Equation 2.1 (Greenberg et al., 1992).

MPN/100 mL = (MPN Index/100 mL) x Lowest dilution ratio (2.1)

### 2.5 Elemental Concentration

Dissolved $Fe(II)_{aq}$, $Fe_{tot}$, $SiO_{2(aq)}$, Ca, and Mg concentration in the experimental fluids were measured spectrophotometrically (Hach Lange DR 2800) (Figure 2.6).


**Figure 2.6:** Hach Lange DR 2800 Spectrophotometer.

### 2.5.1 $Fe(II)_{aq}$ and $Fe_{(tot)}$ analysis

$Fe(II)_{aq}$ and $Fe_{tot}$ in the experimental fluids were measured by following the Ferrozine method. Ferrous Iron Reagent Powder Pillows and Hach FerroVer® Iron Reagent Powder Pillows were used for $Fe(II)_{aq}$ and $Fe_{tot}$ measurements, respectively. For all Fe measurements, 10 mL of diluted samples (ultra-pure water was used for all dilutions) was filled into the special sample tube and the powder pillow ($Fe(II)_{aq}$ or $Fe_{tot}$) was subsequently added. After 3 minutes of reaction time at room temperature, measurements were performed at the absorption value at 510 nm was (Figure 2.7).

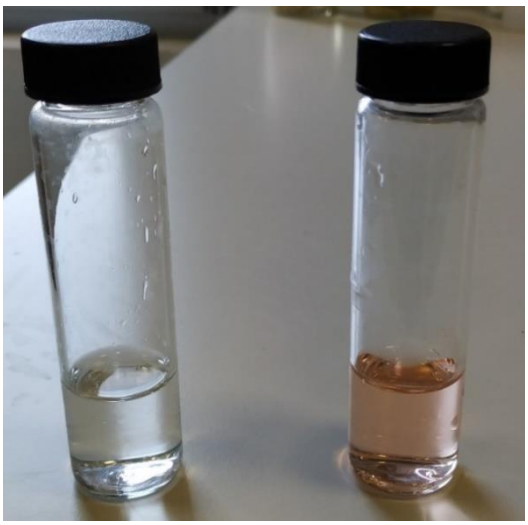

**Figure 2.7:** Spectrophotometric Ferrozine method for $Fe(II)_{aq}$ and $Fe_{(tot)}$ analysis. Redness refers to presence of Fe in the solution.

### 2.5.2 Silica analysis

Silica concentration in the experimental fluids was measured by applying the silicomolybdate method. For these measurements, 10 mL of experimental fluid which was previously diluted for a proper measurement range, was filled into the glass tubes and molybdate reagent was immediately added and the tubes were swirled until the reagent was completely dissolved. Then, an acid reagent was added, and the samples were incubated for 10 minutes at room temperature. Finally, citric acid was added, and the samples were incubated for additional 2 minutes before measurements at 452 nm by HACH DR 2800. Additionally, a blank sample without silica reagents was prepared and used as the standard for the measurements (Figure 2.8).

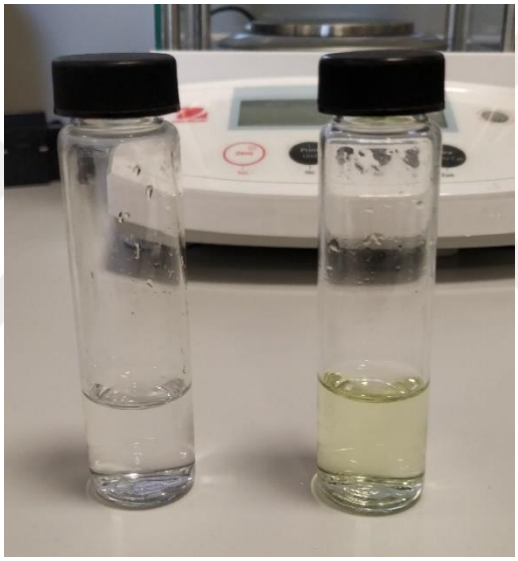

**Figure 2.8:** Spectrophotometric silicomolybdate method for $SiO_{2(aq)}$ analysis. Green color refers presence of $SiO_{2(aq)}$ in the solution.

### 2.5.3 Mg and Ca analysis

Hach LCK 327 chemicals were used to measure Mg and Ca concentrations in the experimental solutions. The chemicals consist of two different solutions: Solution A and Solution B. For these analyses, 4.0 mL of solution A was added to the sample cuvette and after 2 minutes of reaction time, the measurement was recorded. After that, 0.2 mL of experimental solution was added into the cuvette and the subsequent measurement was performed following 30 seconds of incubation time. As a final step, 0.2 mL of solution B was added, and the measurement was performed at 572 nm after 30 seconds of incubation time (Figure 2.9).

**Figure 2.9:** Spectrophotometric measurements for Ca and Mg in the solution.

### 2.5.4 Elemental release rates

To monitor element release kinetic under non-equilibrium conditions similar to those in this thesis linear rate law is frequently used (Wu et al., 2007; Olsson-Francis et al., 2012; Gunes and Balci, 2021). By using similar approach, a linear elemental release rate ($R_i^l$) for each incubation was calculated. Since the total volume of experimental solutions decreased during the course of the experiments equation 2.2 was used to correct the elemental concentration data (Wu et al., 2007):

$$C_{j,i}^{*} = \frac{C_{j,i}(V_0-(j-1)V_s)+\sum_{h=1}^{j-1} C_{h,i}V_s}{V_0} \quad (2.2)$$

where $C^*_{j,i}$ is the corrected dissolved element *i* concentration in the *j*th sampling time, $C_{j,i}$ is the elemental concentration of a given element, $V_0$ is the initial volume of experimental solution in the flasks (0.2 L), $V_s$ is the volume of the aliquot for each sampling (0.005 L for abiotic flasks, and 0.007 L for biological flasks), $\Sigma_{h=1}^{j-1} C_{h,i}V_s$ is the elemental mass of *i* that was extracted during the sampling.

The linear release rates of the elements in the experiments were calculated by Equation 2.3 (Wu et al., 2007):

$$R_i^l = \frac{dC_i^*}{dt}\frac{V_0}{Am} \quad (2.3)$$

where $R_i^l$ is the linear release rate of element *i* (mol $m^{-2}$ $s^{-1}$), $\frac{dC_i^*}{dt}$ is the slope of the line between the corrected elemental concentration that was acquired with Equation 2.2 on

the sampling days $C^*_{i,}$ vs. time, $V_0$ is the initial volume of the experimental solution (0.2 L), $A$ is the BET-$N_2$-specific surface area of the rock grains, and $m$ is the initial mass of the rock grains in an experimental flask.

### 2.6 Mineralogical Characterization of Basalt Samples

The bulk mineralogical compositions of the pre and post reacted BS1 and BS2 rocks along with the secondary products at the end of the incubation were determined with X-Ray diffractometer (XRD) at Istanbul Technical University (ITU) (Figure 2.1a-b). For XRD analysis, each pre-reacted rock sample (ca. 1 g) was crushed and ground in an agate mortar to a powdery size and then thoroughly rinsed with de-ionized water and acetone to remove fine particles. The air-dried post-reacted basaltic grains were crushed and grounded in Retsch RS 200 Grinder at 1250 rpm for 1 minute. Secondary products obtained from the biotic experiments were ground gently in mortars. The obtained powder-sized materials were placed in 0.1 cm size slits and XRD diffractograms were produced by Bruker D8 Advance® Diffractometer with CuKα radiation ranged from 2-72$^o$ and 0.019 intervals. XRD raw data were evaluated by using X'Pert High Score Plus software and the peak values were identified based on X-Ray Powder Diffraction Patterns of Minerals in Clays and Associated Rocks (Chen, 1977).

### 2.7 Scanning Electron Microscopy (EDS)

Morphology and alteration textures of the post-reacted rock grains collected from one of each parallel biotic and abiotic experiments at the end of the incubation time (50 days) were analyzed with scanning electron microscopy with energy dispersive spectroscopy (SEM-EDS). Air-dried basaltic grains were coated with Au/Pd and viewed under SEM-EDS-Philips XL30 ESEM-FEG/EDAX system at Advanced Technologies Research Center, Bosphorus University.

## 3. RESULTS

Four different experimental flasks as biotic and abiotic sets of the BS1 and BS2 were incubated for 50 days. Secondary mineral formation in yellow color was detected in biotic sets (Figure 3.1).

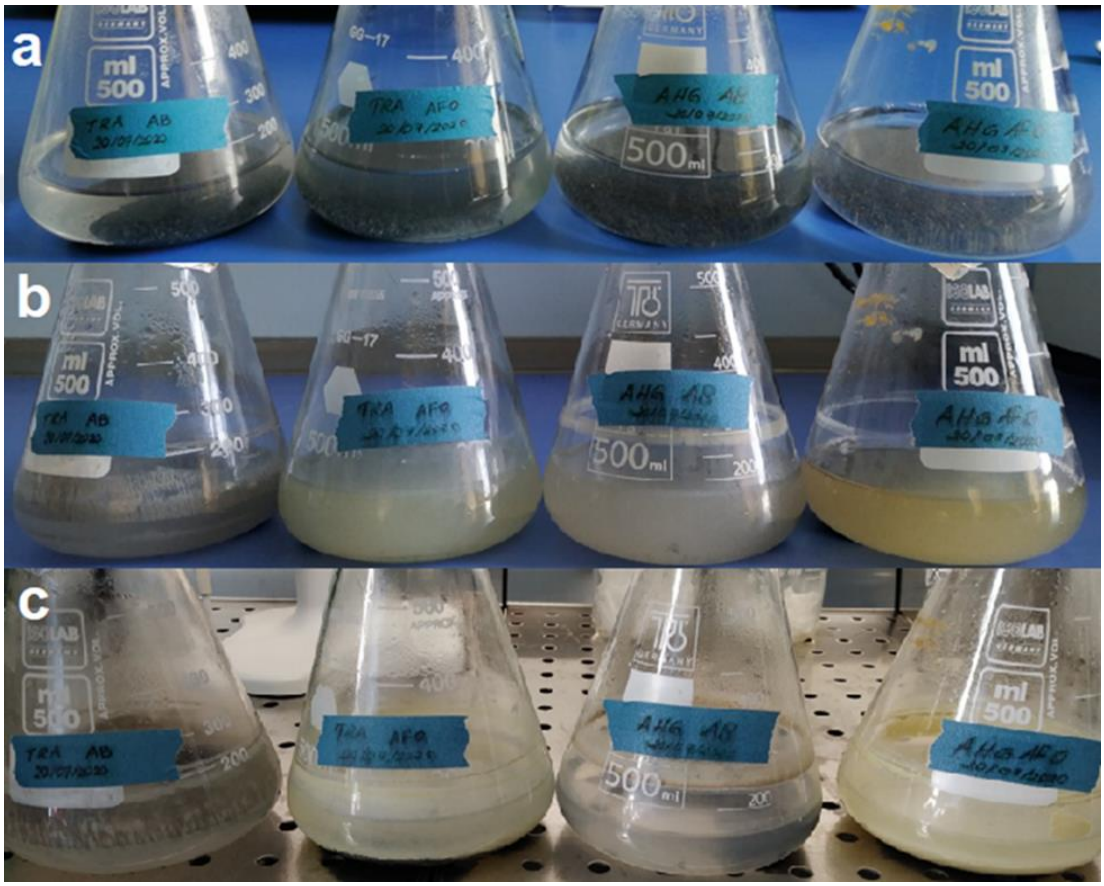


**Figure 3.1:** (a) First day, (b) 25days, and (c) final day of the flasks. From left to right: BS1-AB, BS1-B, BS2-AB, and BS2-B.

### 3.1 Bacterial Growth

The cell numbers of *Acidithiobacillus ferrooxidans* estimated with the MPN assay (Figure 3.2) over the course of the experiments was presented in Figure 3.3. The initial bacterial inoculum used for biotic experiments was estimated as 1.6 x $10^6$ cells/mL and continuously increased, reaching its maximum values on days 15 and 20 in the BS1-B and the BS2-B experiments, respectively. Then, the cell numbers started to decline until day 22 in all biotic experiments and remained almost constant throughout

the entire experimental period. The relatively higher cell number, almost 4 fold higher, was determined in the BS2-B biotic experiments compared to BS1-B experiments. Consistently, dissolved $Fe_{(tot)}$ concentration was nearly 3 fold higher in BS2-B than that in BS1-B experiments.

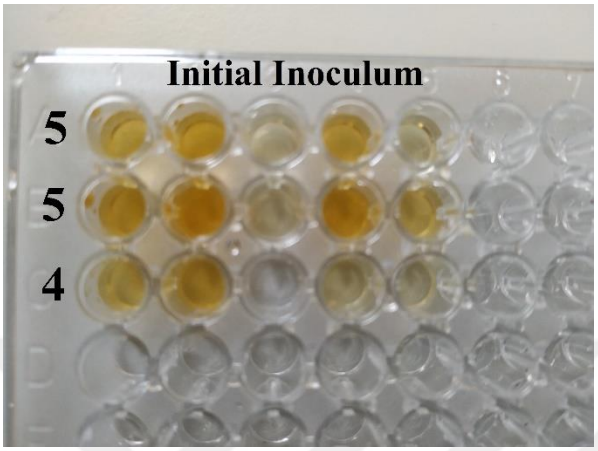


**Figure 3.2:** MPN assay corresponded to the initial stage of the experiments.

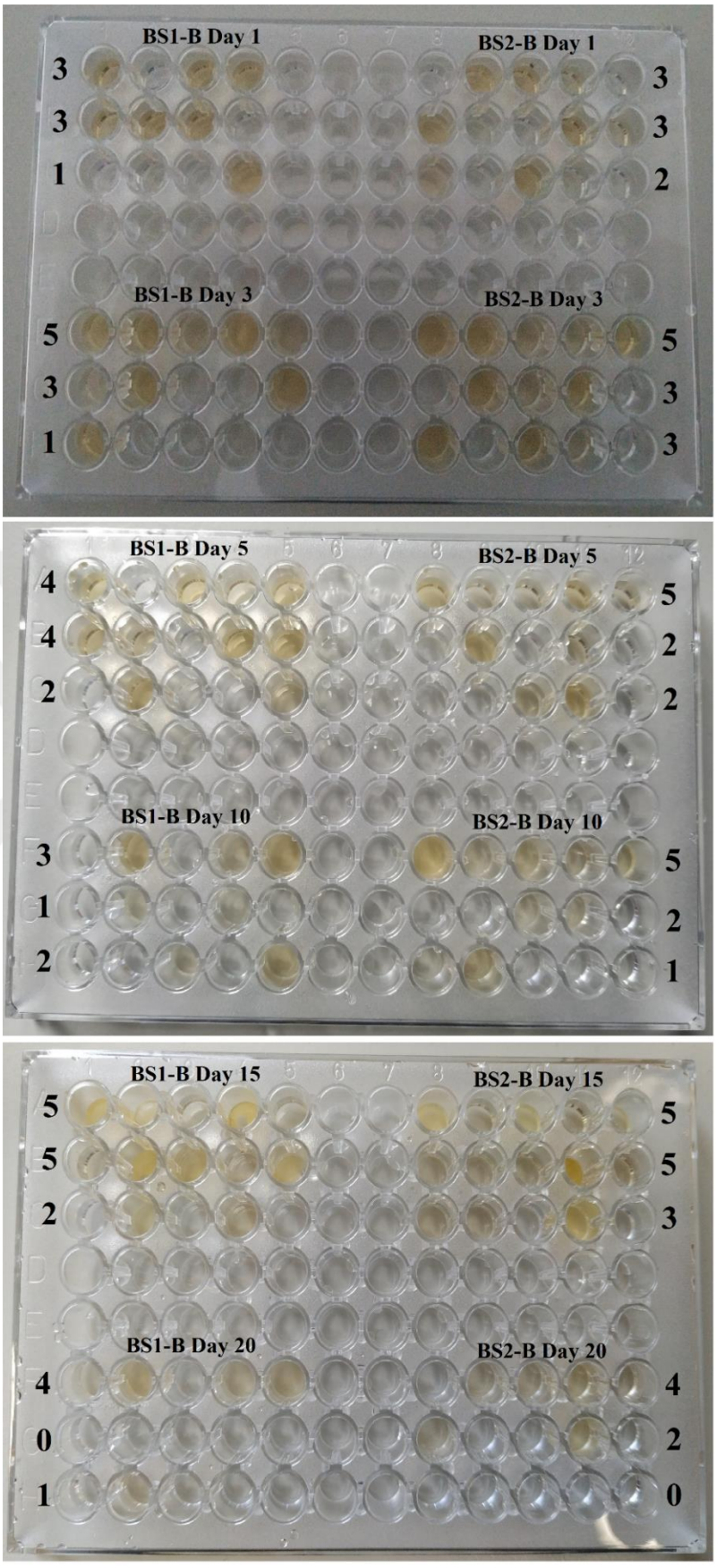


**Figure 3.2 (Continued):** MPN assays corresponded to the different stage of bacterial growth

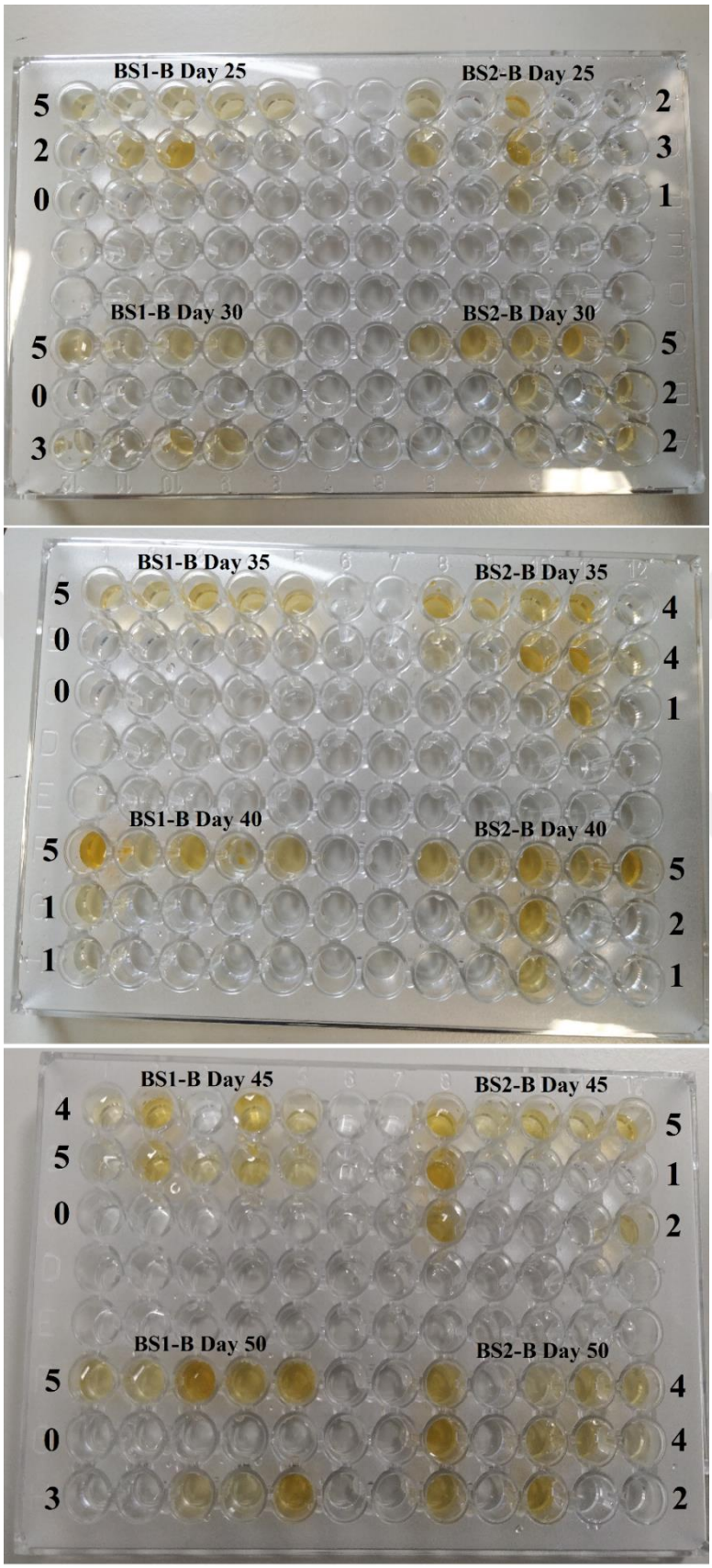


**Figure 3.2 (Continued):** MPN assays corresponded to the different stage of bacterial growth

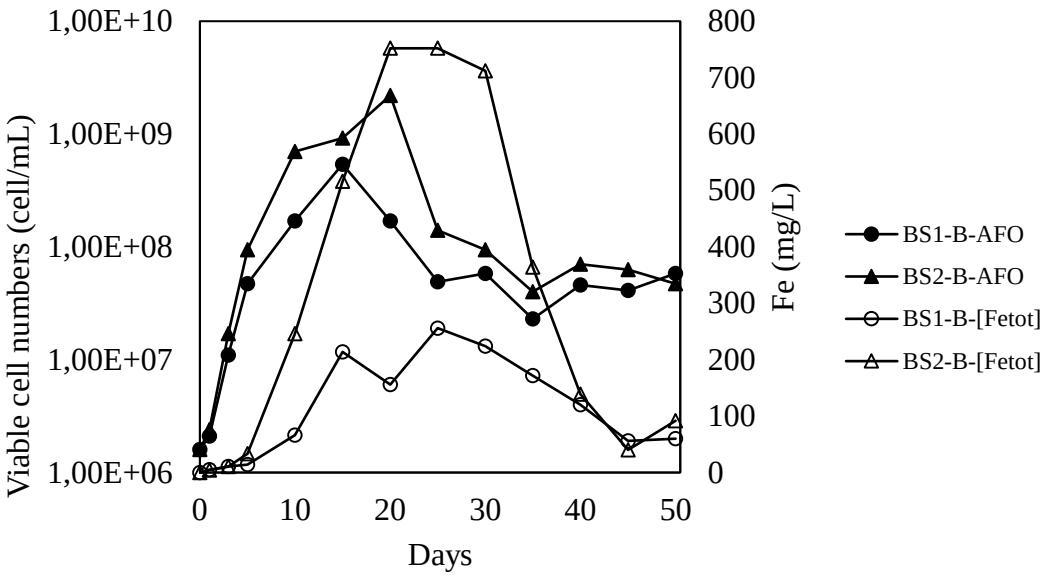


**Figure 3.3:** Viable *A. ferrooxidans* cell numbers (BS1-AFO and BS2-AFO), and dissolved iron concentrations (BS1-$Fe_{(tot)}$ and BS2-$Fe_{(tot)}$) in the biotic sets for 50 days of incubation.

### 3.2 pH Profiles of the Experiments

The pH of each experimental fluid was monitored throughout the experiments. In general, an initial sharp increase in pH was observed under all experimental conditions, reaching 3.7 in the abiotic and 3.2 in the biotic experiments. pH in the biotic flasks was slightly lower than those in the abiotic sets except for BS1-B until days 25. Compared to the pH in the BS1 experiments, pH was lower in the experiments conducted with the BS2 rock sample (Figure 3.4).

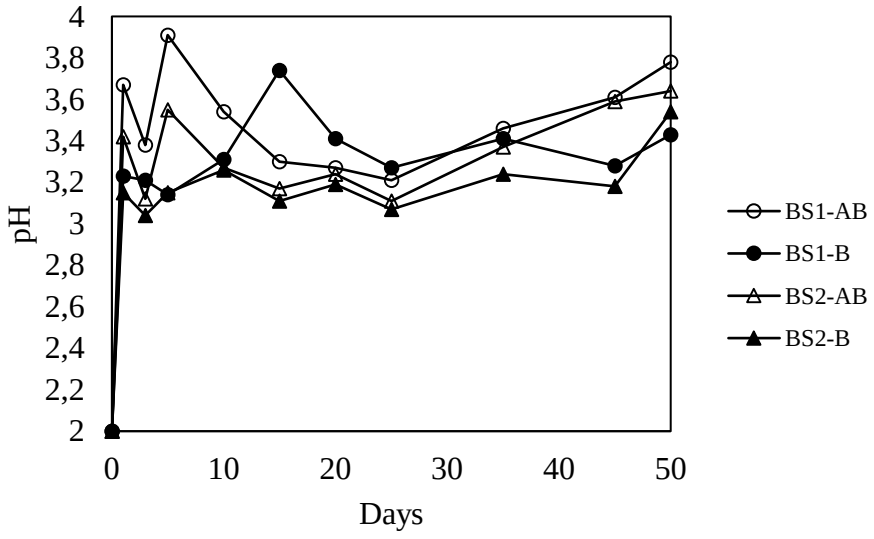


**Figure 3.4:** pH profiles of all experiments during 50 days.

### 3.3 Elemental Concentration in Experimental Solutions

$Fe(II)_{aq}$, $Fe_{(tot)}$, $SiO_{2(aq)}$, Ca, and Mg concentrations in the experimental flasks were continuously monitored throughout the experiments. Fe(II) oxidation rate was calculated for each experimental setup by using the calculated $Fe(III)_{aq}$ and measured $Fe(II)_{aq}$ concentrations at each time point (Table 3.1).

$Fe_{(tot)}$ concentration increased throughout all experiments and reached its maximum value at day 20 following a slight decrease in the abiotic sets while a sharp Fe removal was evident in their biotic counterparts at the end of the experiments (Figure 3.5). $Fe_{(tot)}$ concentration in the abiotic samples was mainly composed of Fe(II) and $Fe(II)_{aq}$ concentration in the biotic sets was noticeably lower (Figure 3.6). Unlike abiotic experiments in which the majority of Fe is in Fe(II) form, Fe(III) is the major Fe form in the biotic samples (Figures 3.5-3.8).

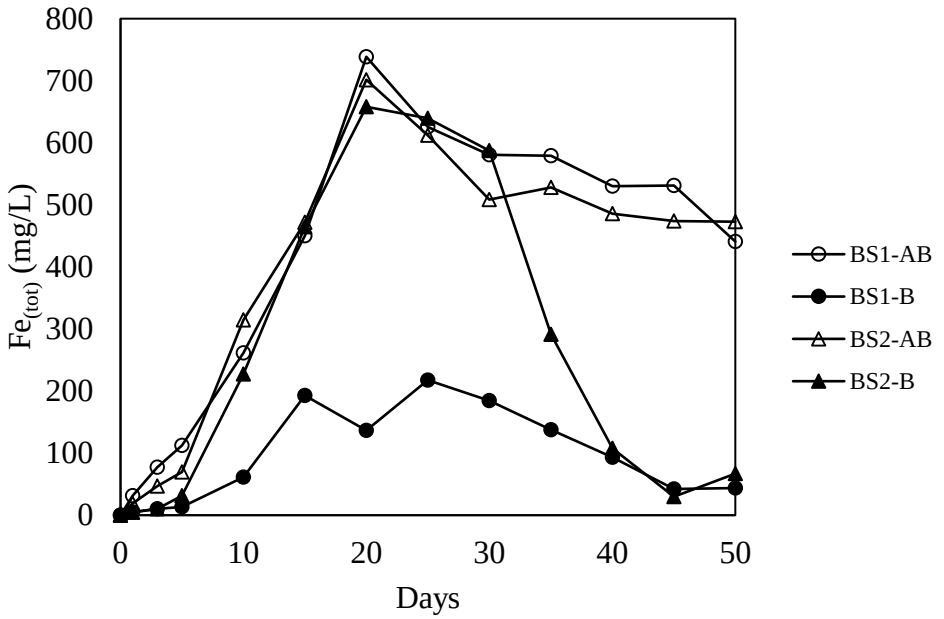


**Figure 3.5:** $Fe_{(tot)}$ concentrations in the experimental fluids during 50 days.

**Table 3.1:** Concentrations of $Fe(II)_{aq}$, $Fe(III)_{aq}$, $Fe_{(tot)}$, $SiO_{2(aq)}$, Ca, and Mg, and oxidixed Fe percentage in the experimental sets during 50 days.

| Experimental Set | Time (days) | $Fe(II)_{aq}$ (ppm) | $Fe_{(tot)}$ (ppm) | $Fe(III)_{aq}$ (ppm) | $SiO_{2(aq)}$ (ppm) | Ca (ppm) | Mg (ppm) | Oxidized Fe (II) (%) |
|---|---|---|---|---|---|---|---|---|
| BS1-AB | 1 | 33,4 | 31,6 | - | 444 | 422 | 96 | - |
| | 3 | 63,96 | 77,22 | 13,26 | 663,01 | 546,01 | 0 | 17,17 |
| | 5 | 106,02 | 112,57 | 6,55 | 788,52 | 744,81 | 103,81 | 5,81 |
| | 10 | 240,5 | 261,31 | 20,81 | 514,31 | 1211,78 | 887,15 | 7,96 |
| | 15 | 381,61 | 450 | 68,39 | 558,01 | 1251,03 | 1037,03 | 15,19 |
| | 20 | 458,51 | 738,52 | 280,01 | 521,51 | 1435,04 | 1443,55 | 37,91 |
| | 25 | 503,21 | 625,61 | 122,4 | 578,01 | 1283,53 | 966,04 | 19,56 |
| | 30 | 567,61 | 580,81 | 13,2 | 297 | 1344,79 | 1478,8 | 2,27 |
| | 35 | 518,41 | 579,21 | 60,8 | 224 | 1400,04 | 942,04 | 10,49 |
| | 40 | 476,64 | 530,11 | 53,47 | 305,35 | 914,52 | 105,11 | 10,08 |
| | 45 | 507,01 | 531,01 | 24 | 217,5 | 1245,04 | 956,04 | 4,51 |
| | 50 | 426,31 | 440,81 | 14,5 | 175,45 | 1312,29 | 802,29 | 3,28 |
| BS1-B | 1 | 3,55 | 5,2 | 1,65 | 444 | 368 | 0 | 31,73 |
| | 3 | 3,31 | 10,14 | 6,83 | 609,39 | 446,56 | 75,96 | 67,35 |
| | 5 | 7,22 | 13,3 | 6,08 | 708,71 | 729,61 | 115,21 | 45,71 |
| | 10 | 14,7 | 61,05 | 46,35 | 469,91 | 1031,4 | 762,28 | 75,92 |
| | 15 | 21,42 | 192,6 | 171,18 | 428,41 | 1233,03 | 1284,54 | 88,87 |
| | 20 | 16,1 | 136,5 | 120,4 | 420,01 | 1505,04 | 1758,26 | 88,2 |
| | 25 | 19,12 | 217,6 | 198,48 | 493,01 | 1802,05 | 2215,57 | 91,21 |
| | 30 | 17,82 | 184,8 | 166,98 | 349,81 | 1716,05 | 1701,56 | 90,35 |
| | 35 | 23,36 | 137,6 | 114,24 | 504,01 | 888,02 | 291,62 | 83,02 |
| | 40 | 21,39 | 93 | 71,61 | 477,41 | 930,03 | 232,22 | 77 |
| | 45 | 3,15 | 42 | 38,85 | 238,5 | 1290,04 | 1188,55 | 92,5 |
| | 50 | 4,49 | 43,5 | 39,01 | 191,4 | 1247,04 | 1708,57 | 89,67 |
| BS2-AB | 1 | 17,7 | 19,2 | 1,5 | 437 | 372 | 0 | 7,82 |
| | 3 | 40,36 | 46,8 | 6,44 | 670,81 | 413,41 | 52,56 | 13,76 |
| | 5 | 93,48 | 69,54 | - | 877,82 | 596,61 | 77,21 | - |
| | 10 | 272,88 | 314,5 | 41,62 | 950,92 | 874,14 | 1192,41 | 13,23 |
| | 15 | 444,61 | 471,61 | 30 | 972,02 | 886,52 | 1604,05 | 6,36 |
| | 20 | 535,51 | 701,52 | 166,01 | 707,02 | 1461,29 | 3062,34 | 23,66 |
| | 25 | 465,81 | 612,01 | 146,2 | 486,21 | 1309,03 | 1986,07 | 23,88 |
| | 30 | 485,11 | 508,21 | 23,1 | 399,31 | 981,77 | 1404,55 | 4,54 |
| | 35 | 473,61 | 528,01 | 54,4 | 371,21 | 888,02 | 1086,04 | 10,3 |
| | 40 | 451,06 | 485,94 | 34,88 | 509,96 | 852,52 | 923,54 | 7,17 |
| | 45 | 483,01 | 474,01 | - | 316,51 | 1305,04 | 1458,56 | - |
| | 50 | 411,81 | 472,71 | 60,9 | 163,85 | 1116,53 | 998,04 | 12,88 |
| BS2-B | 1 | 3,65 | 4,6 | 0,95 | 487 | 318 | 0 | 20,65 |
| | 3 | 2,92 | 10,14 | 7,22 | 663,99 | 419,26 | 19,36 | 71,2 |
| | 5 | 5,98 | 31,5 | 25,52 | 986,12 | 554,81 | 65,81 | 81,01 |
| | 10 | 14,43 | 227,55 | 213,12 | 736,31 | 1049,9 | 1493,05 | 93,65 |
| | 15 | 18,18 | 464,41 | 446,23 | 820,82 | 1548,04 | 2903,69 | 96,08 |
| | 20 | 20,3 | 658,01 | 637,71 | 700,02 | 1715,04 | 3543,61 | 96,91 |
| | 25 | 18,7 | 639,21 | 620,51 | 639,21 | 1564,04 | 2572,58 | 97,07 |
| | 30 | 16,17 | 587,41 | 571,24 | 369,61 | 858,02 | 876,53 | 97,24 |
| | 35 | 12,32 | 291,2 | 278,88 | 318,4 | 1064,03 | 1126,04 | 95,76 |
| | 40 | 8,06 | 107,72 | 99,6 | 385,96 | 852,52 | 1001,04 | 92,46 |
| | 45 | 4,2 | 30 | 25,8 | 273 | 1357,54 | 3206,12 | 86 |
| | 50 | 3,33 | 66,7 | 63,37 | 211,7 | 1312,29 | 2955,61 | 95 |

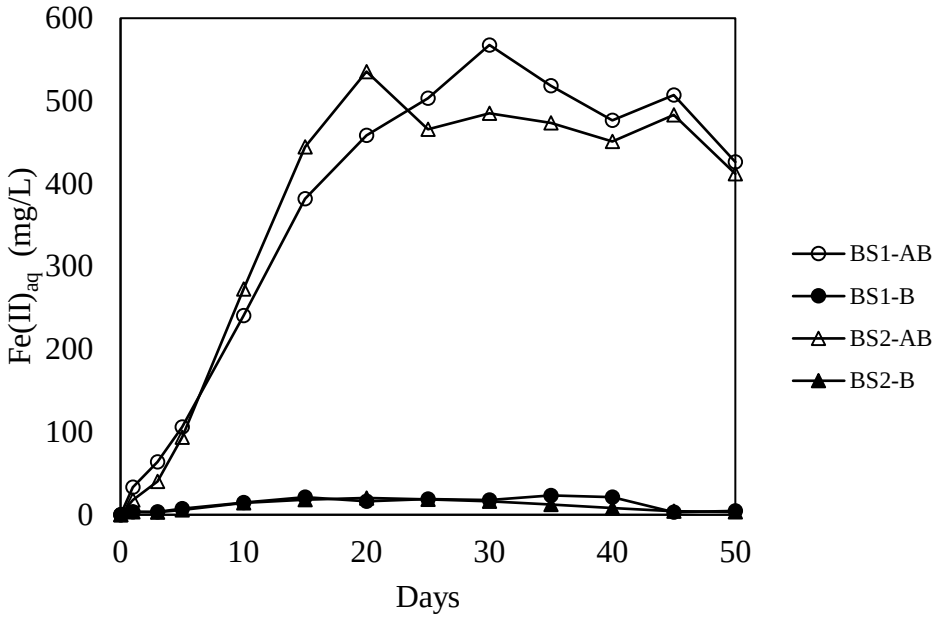


**Figure 3.6:** $Fe(II)_{aq}$ concentrations in the experimental fluids during 50 days.

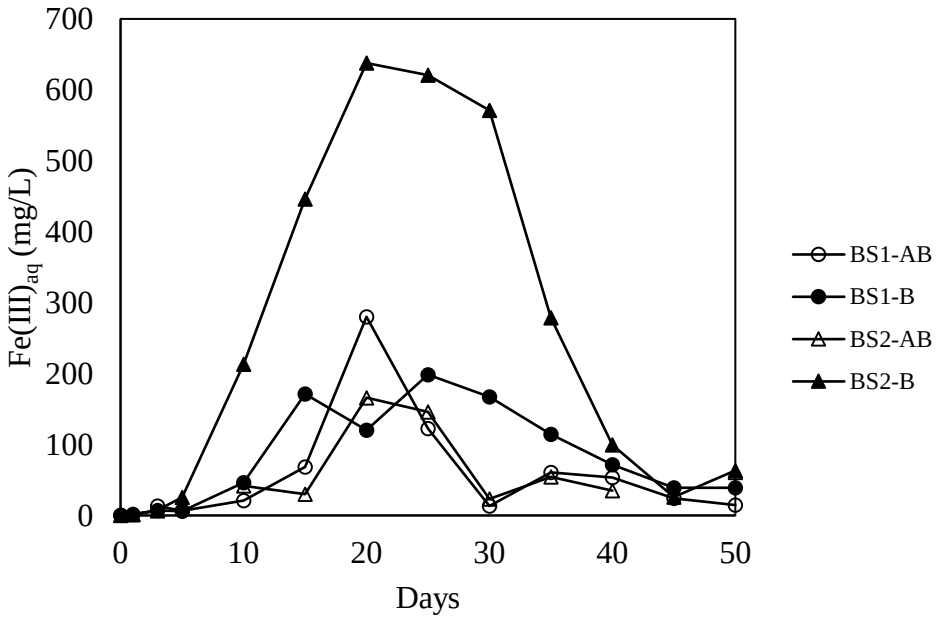


**Figure 3.7:** $Fe(III)_{aq}$ concentrations in the experimental fluids during 50 days.

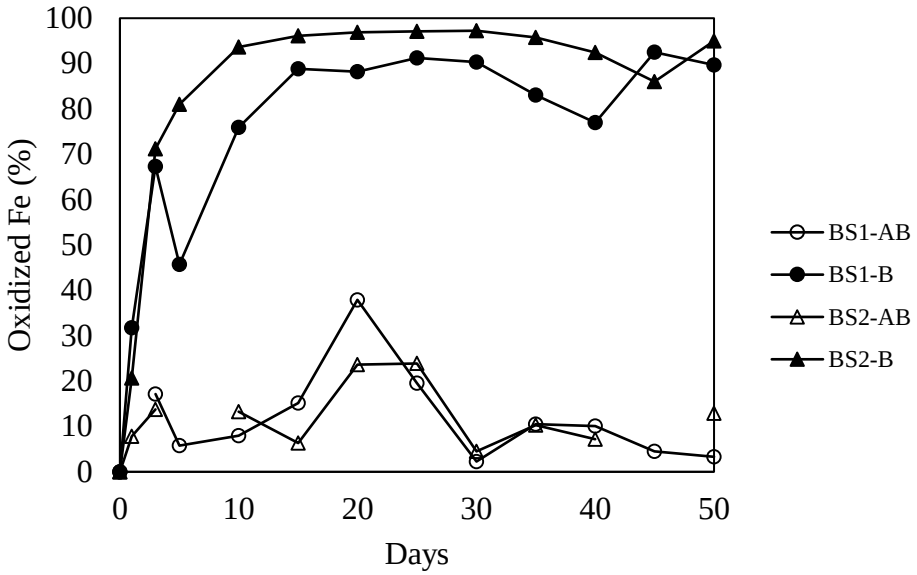


**Figure 3.8:** Percentage of oxidized $Fe(II)_{aq}$ over the course of the experiments.

A rapid initial $SiO_{2(aq)}$ release was observed in all experiments within 5 to 10 days though a relatively higher $SiO_{2(aq)}$ release was present in BS2 basalt experiments. Following a sharp increase and decrease, $SiO_{2(aq)}$ concentration stayed steady until day 25 following continues decreasing and slight increasing trend until the end of the experiments (Figure 3.9). In addition, $SiO_{2(aq)}$ release was lower in biotic sets until day 25. After 50 days of incubation, $SiO_{2(aq)}$ concentration represented quite similar values among the experiments ranging from 163 mg/L to 211 mg/L.

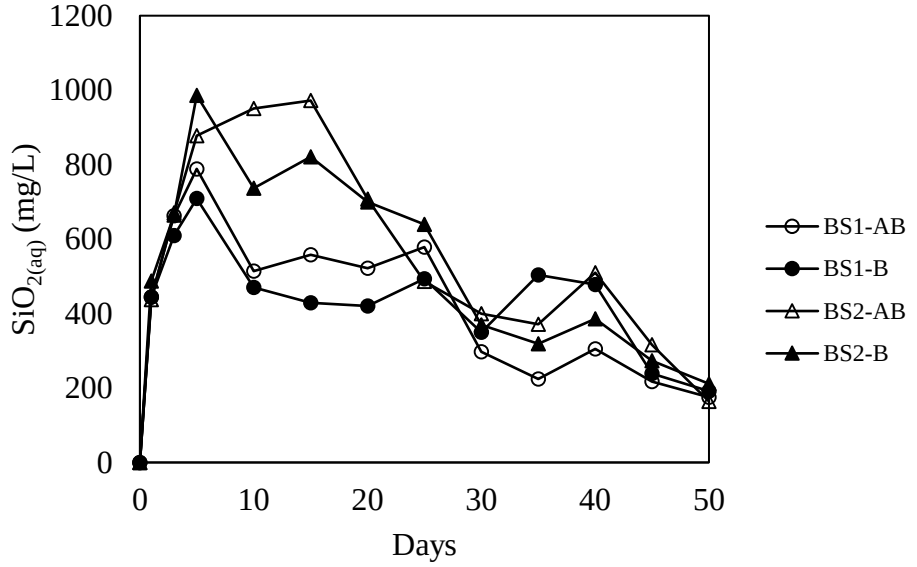


**Figure 3.9:** $SiO_{2(aq)}$ concentrations in the experimental fluids during 50 days.

Compared to $SiO_{2(aq)}$, Ca concentration gradually increased until day 20 reaching its maximum values in biotic experiments except the BS1 experiment showing its maximum values at day 25 as 1800 mg/L. After 25 days, dissolved Ca concentration declined both in the biotic basalt experiments and abiotic BS2 experiments in contrast to abiotic BS1 experiments. In general, although Ca released was slightly enhanced in the biotic experiments its final concentration was similar among the experiments as observed in the $SiO_{2(aq)}$ release kinetics (Figure 3.10).

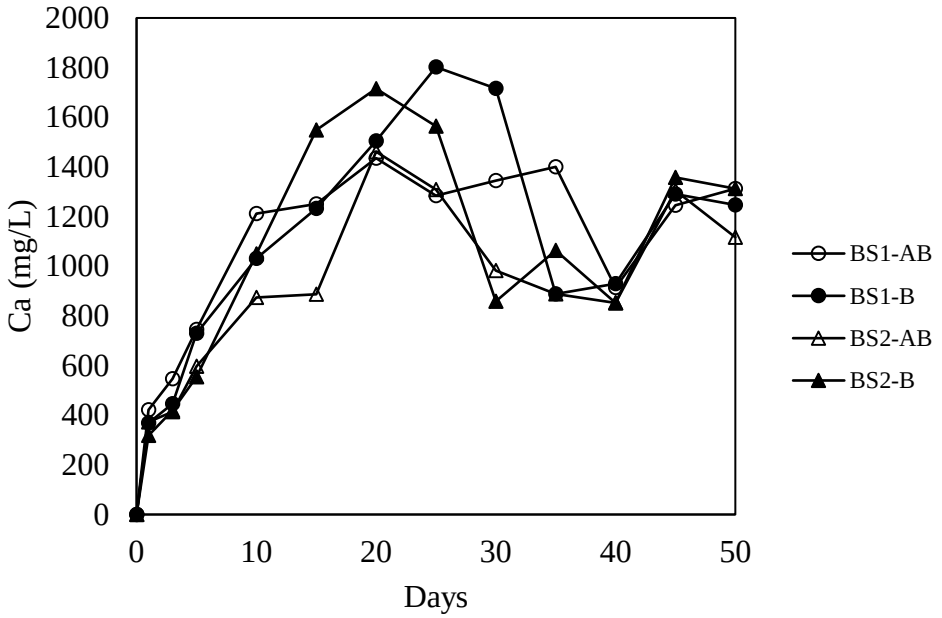


**Figure 3.10:** Ca concentrations in the experimental fluids during 50 days.

Compared to $SiO_{2(aq)}$ and Ca dissolution patterns Mg followed a different dissolution pattern. Mg concentration did not show significant change relative to the initial Mg concentration in the experimental medium for 5 days. Following this step, Mg release in the biotic sets was higher than that in the abiotic flasks, and in the BS2 samples than that in the BS1. After a decrease in all sets until day 40, Mg concentration in the biotic experiments increased sharply and the final concentrations were nearly 1.6 fold higher in the BS1-B sample than that in the BS1-AB and 2.6 fold higher in BS-2 sample than that in the BS2-AB at the end of the experiment (Figure 3.11).

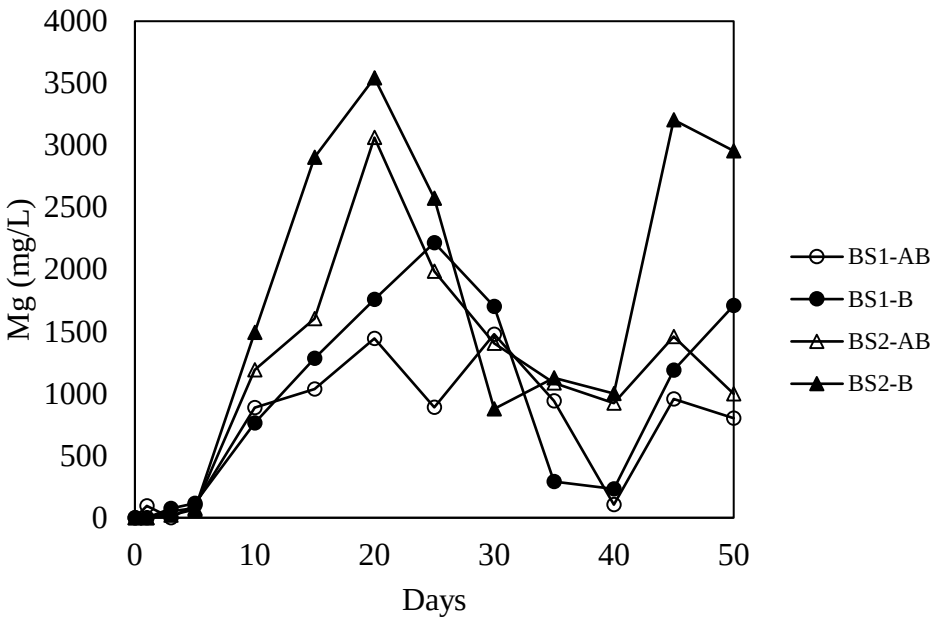


**Figure 3.11:** Mg concentrations in the experimental fluids during 50 days.

### 3.4 Linear Element Release Rates ($R_i^l$)

Elemental release rates for each abiotic and biotic incubation were calculated according to Equation 2.3 (Table 3.2). The linear release rate was only calculated for the initial part of experiments where a linear increase in element concentration as a function of time was measured and no precipitation was unlikely. Nonetheless, it cannot be completely ruled out that a fraction of particularly Fe, released from the rocks, is likely scavenged and/or deposited in the close vicinity of the cell surfaces.

Elemental release rates were calculated for $SiO_{2(aq)}$, Ca, and Mg dissolutions since Fe was precipitated as ferric form as indicated by the experimental results (Figure 3.7). $SiO_{2(aq)}$ release rates showed slight differences in the biotic and abiotic sets of basalts but higher in the BS2 compared to BS1 rock. This was clearly evident in the Mg release rate which is significantly higher in the BS2 experiments regardless of experimental conditions. Mg release rate was 1,23 and 1,15 fold higher in BS1 and BS2 biotic experiments, respectively. Ca release rates were very similar for biotic and abiotic samples in BS1 rock sample, but the release rate in BS2-B was 1,17 fold was higher than those in BS2-AB. In addition, release rates for all $SiO_{2(aq)}$, Ca, and Mg were higher in BS2 samples than those in BS1.

**Table 3.2:** Elemental release rates ($R_i^l$) of $SiO_2$, Ca, and Mg from the experimental sets using Reaction 2.3 (x $10^{-12}$ mol/$m^2$/s).

| Experiments | $R_{SiO2}$ | $R_{Ca}$ | $R_{Mg}$ |
|---|---|---|---|
| BS1-AB | 3,699 | 2,527 | 4,179 |
| BS1-B | 3,304 | 2,539 | 5,148 |
| BS2-AB | 4,359 | 2,721 | 9,405 |
| BS2-B | 4,897 | 3,196 | 10,883 |

### 3.5 Microscopic Analyses of Alteration Texture Morphology of the Post Reacted Basalt Grains

SEM images of the pre and post reacted basalt grains are presented in (Figures 3.12-14) and are further compared to surface images of the basalts obtained from the abiotic experiments to reveal surface changes associated with the bacteria as well as possible precipitation of secondary phases/minerals (Figure 3.12). Compared to the surface of the pre-reacted basalt, a thick alteration layer is present on the surface of the basalt grains in all the experiments (Figures 3.13a-14). These continuous surface altered layers are more evident in the abiotic experiments and highly fractured and detached from the underlying surface (Figure 3.13b, c, d). There might be two reasons for the observed fractures. Precipitation of secondary phases replaces the primary materials and replacement reactions generally involve volume changes such expansion and shrinkage generating stress that causes fracture between the product and the primary materials (Ruiz-Agudo et al., 2014). It is equally possible that desiccation during SEM imaging may partly contribute to these structures. However, differences observed in the biotic and abiotic samples suggest that desiccation may play an insignificant role, if occurs, during the fracture development.

The altered regions in the biotic experiments did not show any imprints fitting in size to the cells. SEM images showed that the bacteria do not seem to colonize the surface of the rock particles either and moreover there was no obvious sign of the cell attachment to the surface (Figure 3.14). However, in contrast to the abiotic experiments, SEM images revealed clustered poor spherical phases with sizes ranging from less than 1 μm or higher on the basaltic grains obtained from the biotic experiments (Figure 3.14d). EDX pattern of these phases indicated Fe and O enrichments with sulfur (Figure 3.14e). These phases, at least in part, may explain the

decreasing release patterns of Fe in the biotic experiments. Consistently, comparative EDX patterns of the spherical phases obtained from the surface of the post-reacted rocks revealed Fe and S enrichments (Figure 3.15). In contrast to elemental surface enrichments, mineralogical compositions of the post-reacted rock grains showed no significant mineralogical changes with the extent of the reactions, indicating congruent dissolution characteristics, at least within the period of the current experimental time.

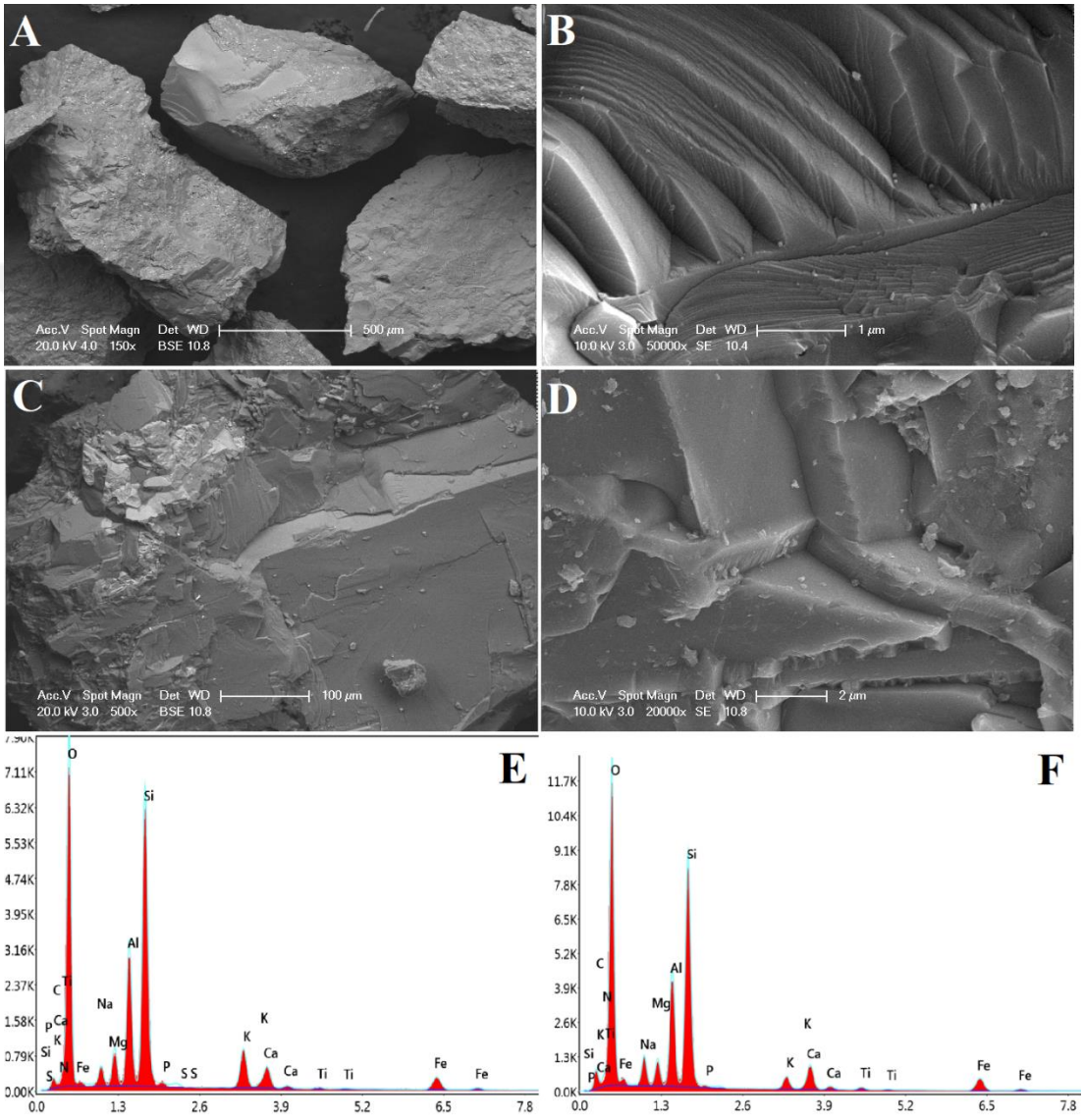


**Figure 3.12:** SEM images of (A) and (B) Pre-reacted BS1 grains, (C) and (D) pre-reacted BS2 grains. EDS analyses of (E) BS1 and (F) BS2.

Multiple EDS point analyses averaged to obtain an average composition for the pre and post-reacted basaltic grains were used to compare changes in surface chemistry of the basaltic rocks. A comparative EDS spectrum of the basaltic grains obtained from all the experiments is presented in Figure 3.15. The surface of the post-reacted basaltic

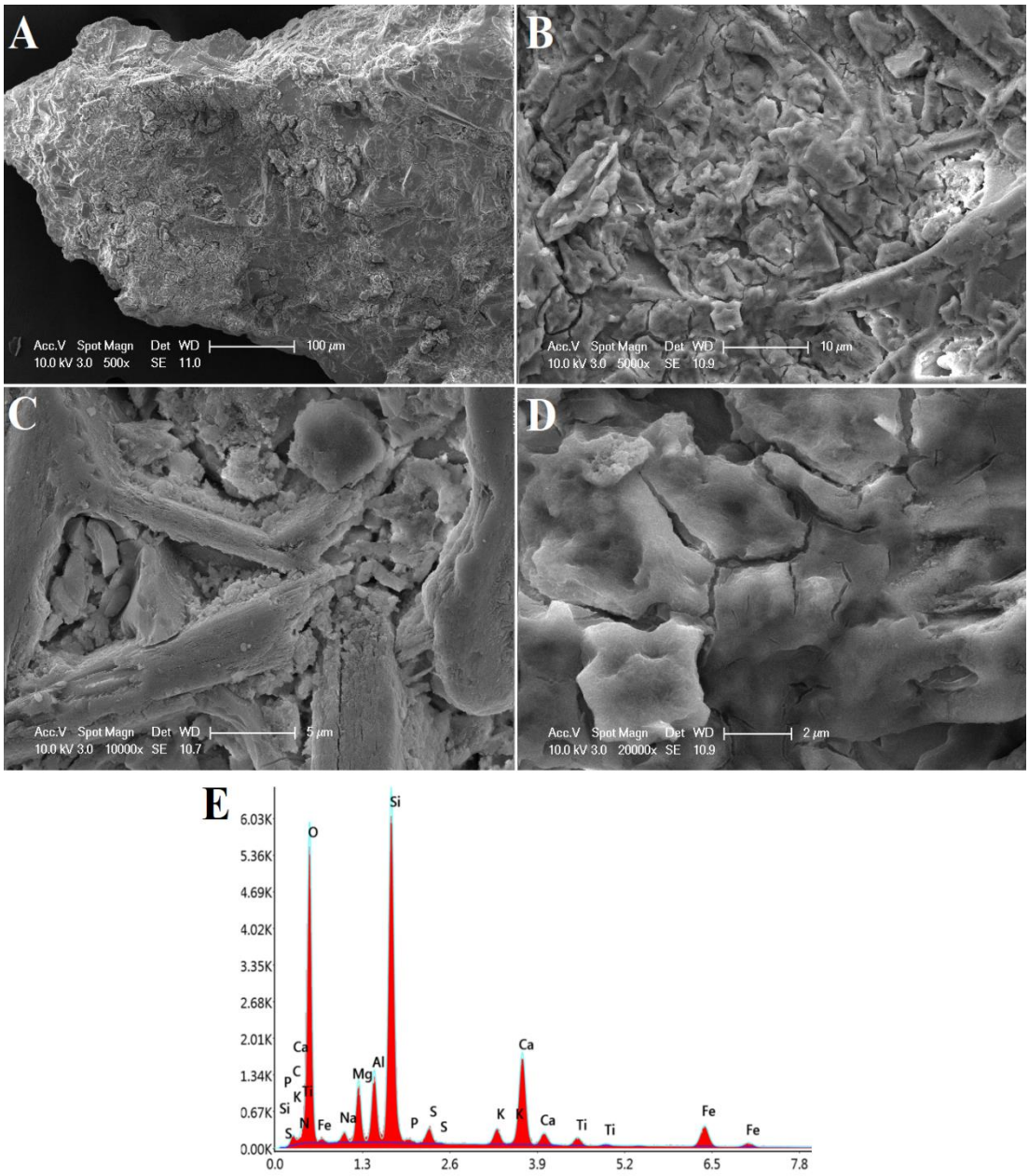


**Figure 3.13:** SEM images (A-D) and EDS analysis (E) of basalt grains from BS1-AB.

grains in the biotic experiments exhibits a significant increase in Fe and S compared to the pre-reacted basaltic grains as well as those in the abiotic experiments. Consistently, Ca enrichment is present in abiotic experiments relative to the pre-reacted basaltic grains. Al increase is also present in the biotic experiments but less dramatically. A decrease in Si, Ca, Na and Mg were measured in the biotic experiments. A slight Si enrichment is present in the abiotic experiments relative to the pre-reacted rock particles. K decrease was detected in abiotic experiments while it increased in biotic flasks.

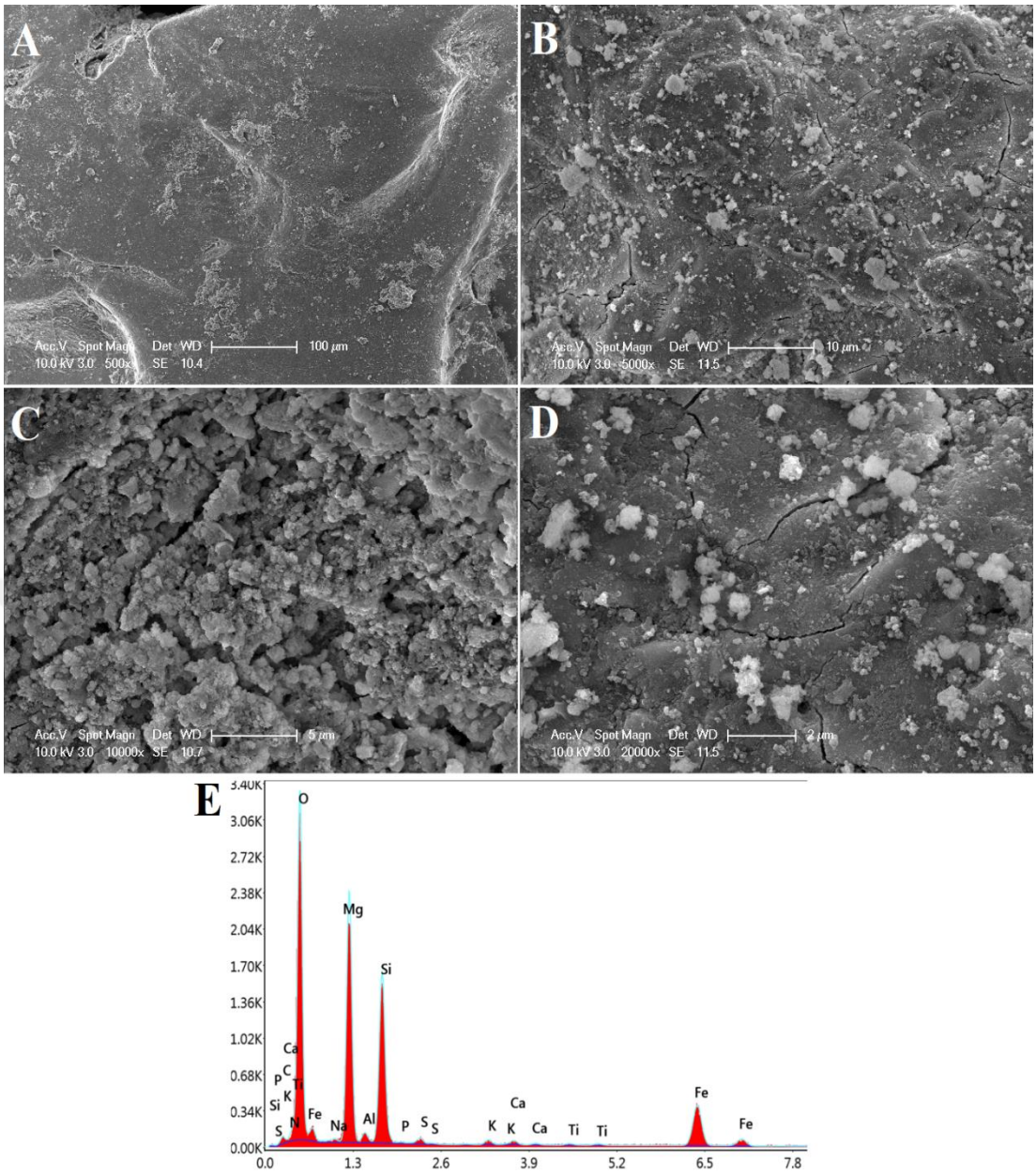


**Figure 3.14:** SEM images (A-D) and EDS analysis (E) of basalt grains from BS2-B.

EDS spectra showed that divalent cations $Ca^{2+}$ and $Mg^{2+}$ were enriched in the abiotic samples while trivalent cations $Fe^{3+}$ and $Al^{3+}$ ratio were higher in the biologically-weathered basaltic grains. Fe, Al, S, and K enrichment and Ca and Mg depletion were the main difference between the two conditions.

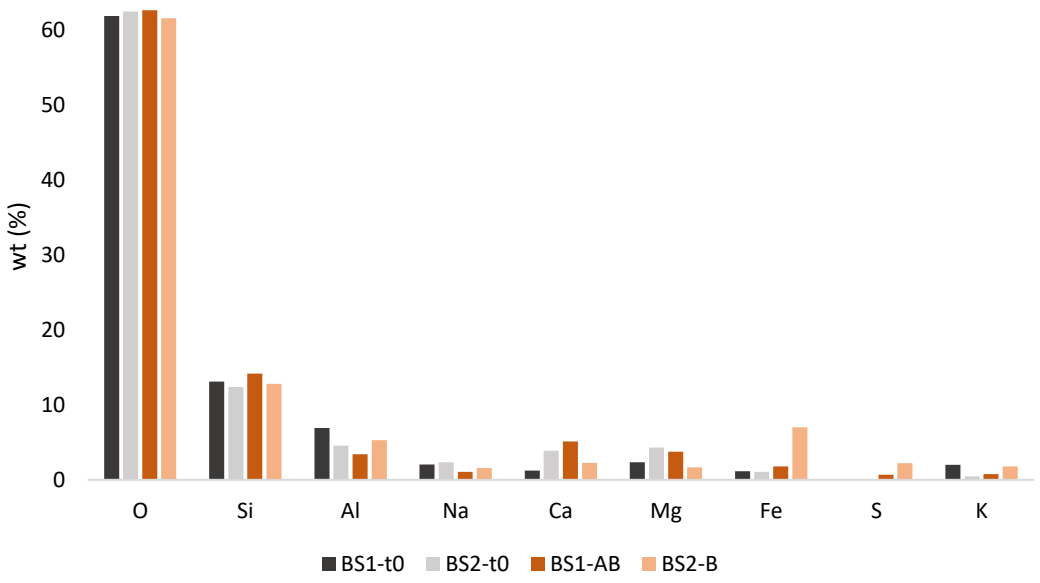


**Figure 3.15:** Weight percentages of the element presence (O, Si, Al, Na, Ca, Mg, Fe, S, and K) in the EDS analyses of pre and post-reacted basalt grains.

EDS mapping was also applied for the pre-reacted and post-reacted grains (Figures 3.16-18. Consistent with EDS measurements, significant Fe enrichment was only observed in the BS2-B basalt experiments (Figure 3.18). Besides Fe, there was no significant enrichment of released elements on the surface of the basaltic samples. Moreover, the surface chemistry of the pre and post-reacted basaltic rocks resembles a similarity with homogenous elements distribution. Nevertheless, Ca, Mg, Al, and Fe presence on the BS2-B grains was greater than those in the BS1-AB grains, indicating biological influences on the enrichment of these elements in the solid phases.

### 3.6 Mineralogical Analysis of Basalt Grains and Precipitates

Mineralogical compositions of the post-reacted basalt grains as well as the secondary precipitations obtained at the end of the biotic experiments were determined by XRD analysis (Figure 3.19). There are no significant mineralogical differences between the pre and post-reacted basalt grains. Clay phases were identified in BS2-B. The only difference was the decrease in the peak strength in the post-reacted grains, likely indicating a change in the amount of the respected minerals and/or presence of amorphous phases (Figures 2.1 and 3.19).

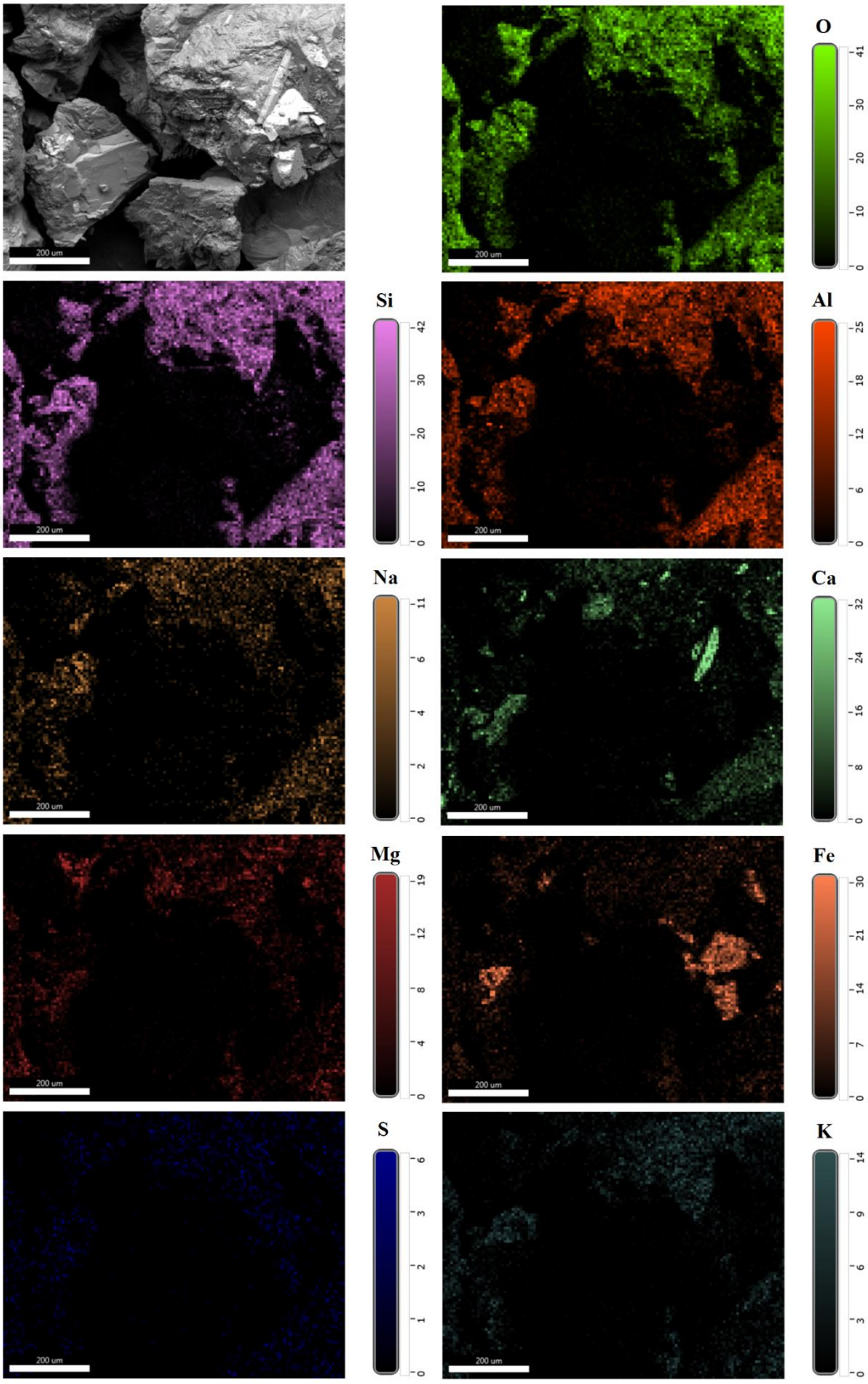


**Figure 3.16:** EDS mapping of the BS1 grains before the experiment.

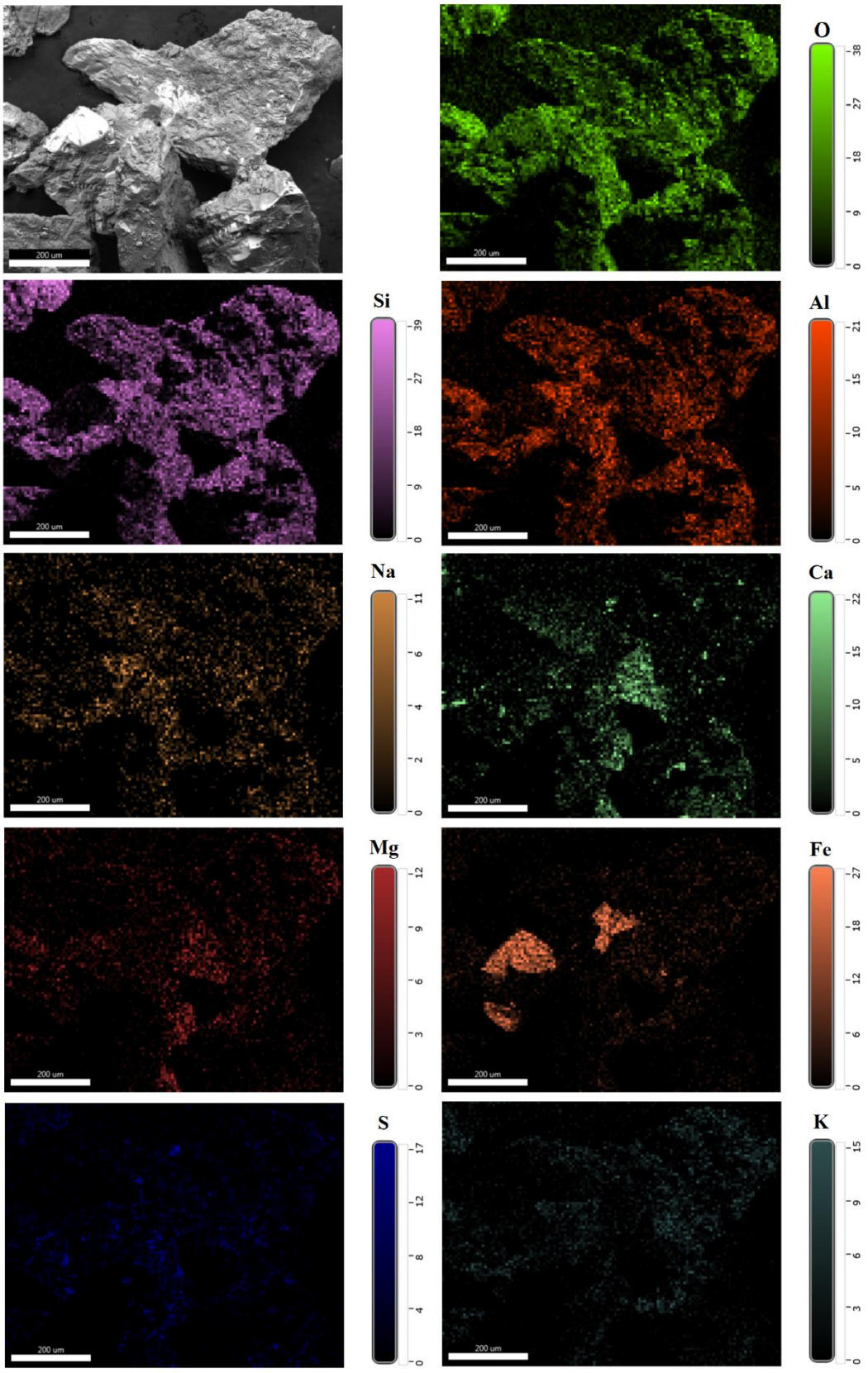


**Figure 3.17:** EDS mapping of the BS1-AB grains.

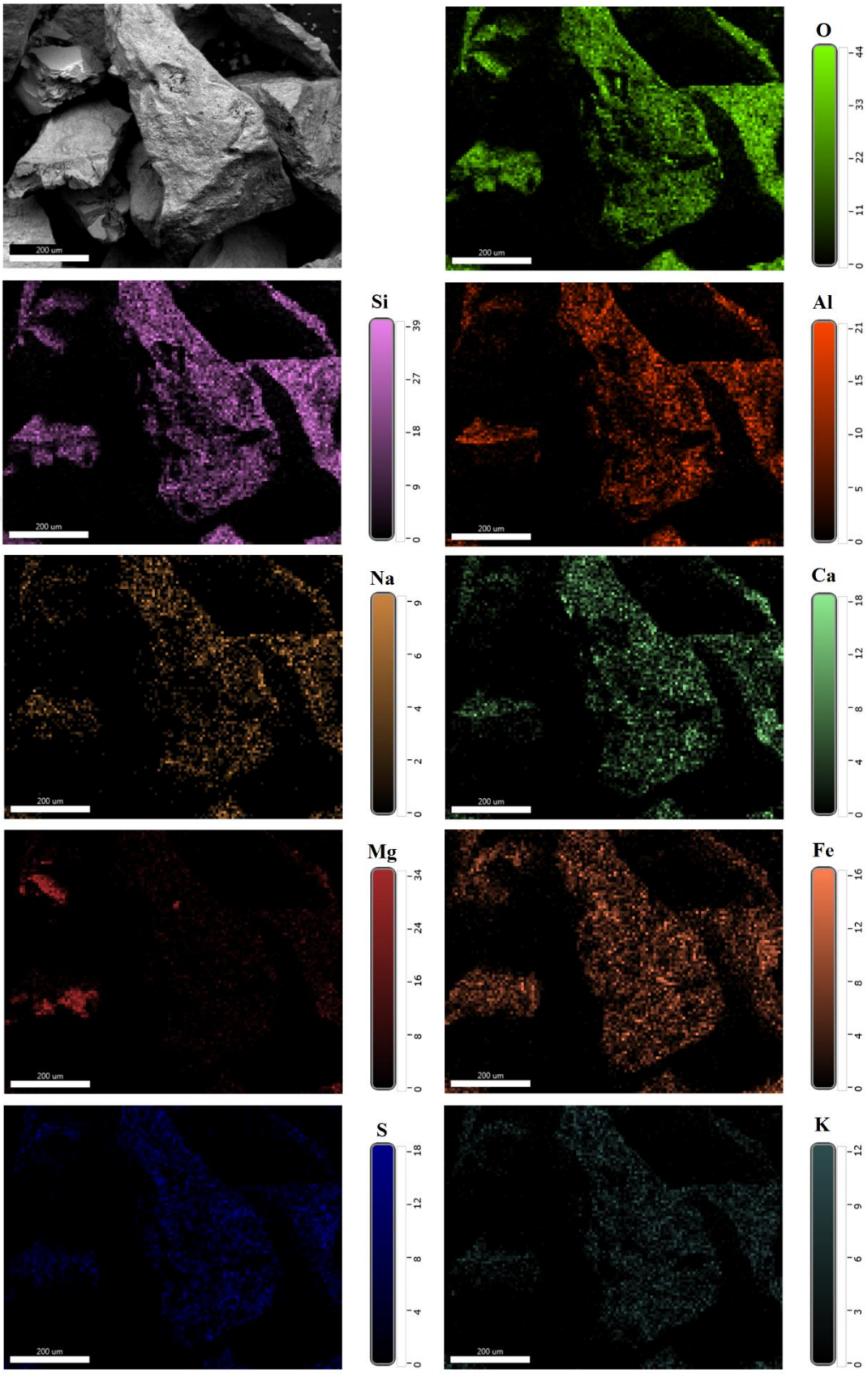


**Figure 3.18:** EDS mapping of the BS2-B grains.

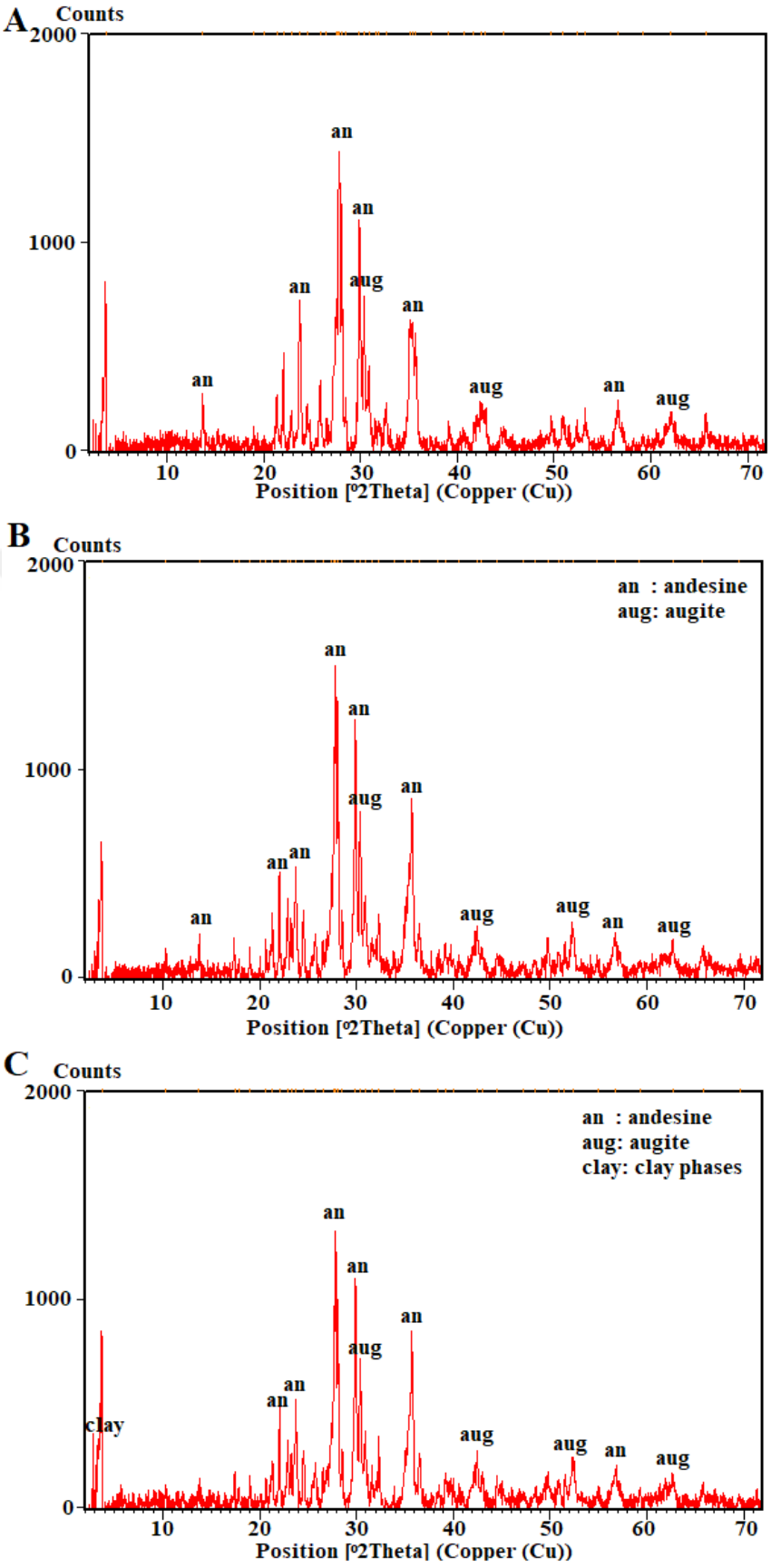


**Figure 3.19:** Mineralogical compositions of surface of the post reacted basalt grains in (A) BS1-AB, (B) BS2-AB, and (C) BS2-B experiments.

Yellow precipitations observed in both biotic experiments were collected for XRD analysis XRD analysis showed the existence of Fe-sulfate mineral jarosite ($(K,Na,H_3O)Fe^{3+}_3(SO_4)_2(OH)_6$) and Ca-sulfate mineral gypsum ($CaSO_4.2H_2O$) with clay mineral (Figure 3.20).

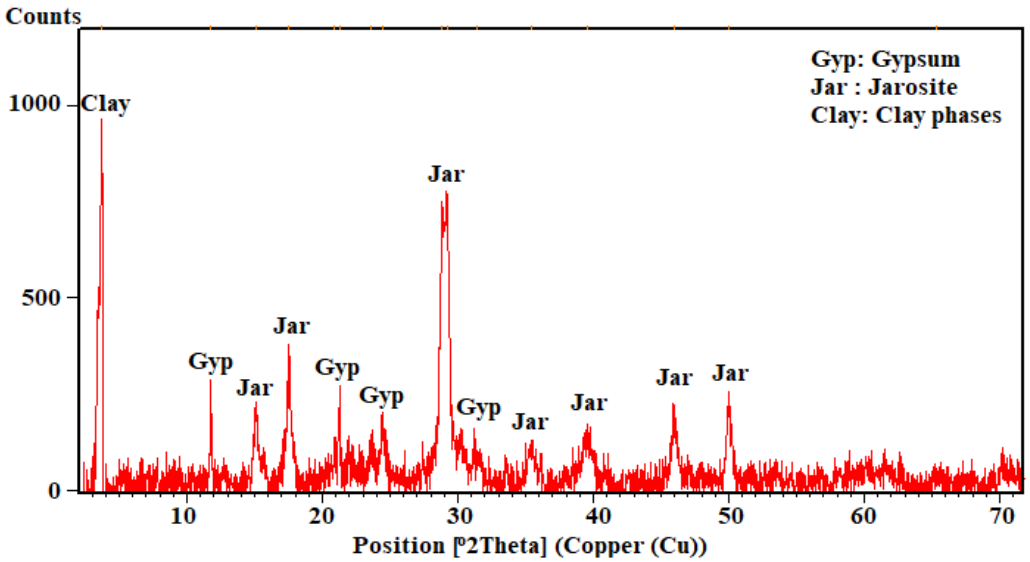


**Figure 3.20:** Mineralogical composition of the yellow precipitate in the BS2-B sample.

## 4. DISCUSSION

The basalt dissolution experiments performed in the presence and absence of *A. ferrooxidans* demonstrated that biotic reactions did not significantly affect the dissolution of basaltic rock under the current experimental conditions. This is particularly evidenced by the similar elemental dissolution rates calculated for the rocks (Table 3.2). The experimental results also revealed that the cells are not found on the rock surfaces under acidic conditions (Figure 3.13). Thus, there was no measurable difference in the amounts of major elements released in the experiments with *A. ferrooxidans* than those in abiotic experiments. Even though silica, calcium, magnesium leaching rates from the basaltic grains did not show significant differences among the biotic and abiotic experiments, the extent of Fe released was greater in the biotic systems, particularly in the BS2 sample. This likely indicates that $Fe(II)_{aq}$ leached from the basaltic grains was immediately biologically oxidized by *A. ferrooxidans*, and precipitated as jarosite and Fe-oxyhydroxides causing a change in the equilibrium of the experimental solution favoring further dissolution of the rocks (Figure 3.8) while $Fe(II)_{aq}$ in the abiotic experiment was accumulated in the solution.

The increasing number of the cell from $1.6 \times 10^6$ cells/mL to $5.4 \times 10^8$ cells/mL for the BS1-B sample and to $2.2 \times 10^9$ cells/mL for the BS2-B sample over the entire course of the experiments suggest that dissolution of basaltic rocks support not only the survival of the cells but also the growth of the cell under acidic conditions. The maximum Fe ion concentration coupled with the higher cell number in the BS2-B sample relative to the BS1-B sample implies the mineralogical influences on the dissolution rate of the basalts.

### 4.1 Basalt Dissolution and Elemental Release

$Fe_{(tot)}$, $Fe(II)_{aq}$, $SiO_{2(aq)}$, Ca, and Mg concentrations in the experimental solutions as a result of the interaction between basalt grains and water in both abiotic and biotic conditions were investigated. Numerous laboratory-based studies revealed that microorganisms may have an accelerating or inhibiting effect on the dissolution of silicate rocks/minerals, elemental release, and the enrichment of elements within the

secondary mineral formations (Vandevivere et al., 1994; Olsson-Francis et al., 2012, 2017; Stockmann et al., 2012; Garcia et al., 2013; Perez et al., 2016; Barker et al., 2019; Lamérand et al., 2020; Gunes & Balci, 2021).

At the end of the experiments, $Fe_{(tot)}$ and $Fe(II)_{aq}$ concentrations were higher in the abiotic samples compared to biotic sets (Figure 3.5). However, Fe enrichment on the surface of the post-reacted basalt samples along with the formation of Fe containing secondary phases implies a solution saturated with Fe(III) phases. Moreover, oxidation of nearly 90% of the $Fe(II)_{aq}$ to $Fe(III)_{aq}$ in the solution provides further evidence for bacterial activity regulating basalt dissolution via Fe(II) oxidation (Figure 3.8).

$SiO_{2(aq)}$ concentration in the solutions was solely originated from the dissolution of the silicate minerals in the basaltic grains. The concentration of $SiO_{2(aq)}$ was lower in the biotic sets than that of their abiotic counterparts until day 25, but the final concentration was similar among all sets as indicated by the similar Si release rate calculated for each experiment (Table 3.2). Santelli et al., (2001) showed that *A. ferrooxidans* reduced the Fe-silicate mineral fayalite dissolution. Additionally, Welch and Banfield (2002) stated that *A. ferrooxidans* metabolism gave rise to the laihunite-like layer formation on the olivine surface and thus caused the inhibition of the olivine dissolution by creating a barrier effect between mineral surface and water. Similar dissolution rates calculated for the biotic and abiotic experiments are corroborated with the results of Welch and Banfield (2002) and Santelli et al., 2001. This similarity is due to Fe oxidation and its further precipitation of the secondary phases both in the biotic and abiotic solution as indicated by the secondary Fe formation particularly in the biotic experiments. Likely, the amount of the secondary Fe phases in the abiotic experiments was low to detect with XRD (< 3 %). A good correlation exists between Fe and Si release behavior that seems to be consistent (Figure 3.5 and 3.9).

Ca and Mg concentrations in the fluids at the end of the experiments were higher in the biotic experiments. Mg concentrations were 1.6 and 2.6 fold higher and Ca were 1.25 and 1.17 fold higher in the BS1 and BS2 biotic experiments, respectively. Under acidic conditions, release rates of Mg and Fe from the crystalline basalt are higher than the other cations (Gudbrandsson et al., 2011). There are two possible reasons for the enrichment of Ca and Mg in aqueous solutions despite the similar silicate dissolution in the biotic flasks: (1) The preferential dissolution of Ca and Mg from the basaltic

grains by *A. ferrooxidans* activity, or (2) Ca and Mg precipitation in the abiotic flasks. Trivalent cations such as $Fe^{3+}$ and $Al^{3+}$ have more affinity than divalent cations $Ca^{2+}$ and $Mg^{2+}$ to form sulfate minerals under acidic conditions (Bigham & Nordstrom, 2000; McCollom et al., 2013). Thus, the second probability looks contingent on the experimental situation.

The secondary precipitation in yellow color identified as jarosite in addition to gypsum, Ca-sulfate mineral, in the biotic flasks are likely resulted from *A. ferrooxidans* metabolic activity causing oxidation of Fe(II) to Fe(III). Jensen and Webb (1995) stated that when the ferrous iron is oxidized under acidic conditions with the presence of sulfate ions, ferric hydroxysulfates form where M is $Na^+$, $K^+$, $Ag^+$, $NH_4^+$, or $H_3O^+$ (Reaction 4.1).

$$3Fe^{3+} + M^+ + 2HSO_4^- + 6H_2O \rightarrow MFe_3(SO_4)_2(OH)_6 + 8H^+ \quad (4.1)$$

EDS spectra demonstrated Fe and S enrichment in the solid phase on the post-reacted basalt grains in BS2-B (Figures 3.15 and 3.18). Also, the sharp decrease in Ca concentration in biological samples after days 25 and 30 may be explained by gypsum formation (Tosca et al., 2004). Similarly, Dopson et al., (2009) indicated jarosite and gypsum formation by *A. ferrooxidans* metabolism during augite dissolution.

Linear release rates were calculated for the first days of the experiment to catch the linear rate of the elemental dissolutions, and to limit the formation probability of the secondary precipitations. However, the elemental uptake of the Ca and Mg by bacterial cells could have affected the release rate (Balci & Demirel, 2016). $R_{Ca}$ and $R_{Mg}$ were higher and $R_{SiO2}$ was lower in the BS1 biotic experiments. $R_{SiO2}$, $R_{Ca}$, and $R_{Mg}$ were greater in the biological set than those in the abiotic flask for BS2. BS1 and BS2 rocks both contain andesine and augite, but Ca composition was greater in BS1, and Mg and $SiO_2$ composition was higher in BS2. Also, rock crystallinity is one of the factors that affect dissolution (Wolff-Boenisch et al., 2006). Thus, the difference in the dissolution rates between two basalt samples could be related to the rock crystallinity and/or elemental composition.

### 4.2 Microbial Influences on pH Changes

The pH of the solutions was kept under 3.0 by sulfuric acid addition to (1) prevent spontaneous oxidation of Fe(II) which dissolved from the basaltic grains, and (2) to

maintain acidic conditions for the growth of *A. ferrooxidans* bacteria. Ferrous iron oxidize spontaneously under pH conditions higher than 3.0 (Morgan & Lahav, 2007). Because there is no sulfur source in the BS1 and BS2, $Fe(II)_{aq}$ was the only source for the growth of bacteria. Acidification of the solution provides the availability of $Fe(II)_{aq}$ for *A. ferrooxidans.* In the natural habitat of *A. ferrooxidans,* AMD sites, the acidic condition is provided by a sulfuric acid formation which is resulted by the sulfide oxidation (Akcil & Koldas, 2006). Therefore, sulfuric acid was added to the experimental sets.

Silicate mineral dissolution induces the drawdown of $CO_2$ in the water and results in an increase towards neutral values (Hartmann et al., 2013). When the cations are released from the silicate minerals into the aqueous solutions, hydronium ions react with these cations. Substitution reactions between hydrogen ions and the cations in the silicate minerals cause not only a rapid release of the cations to the solution but also an increase in pH (Reactions 4.2 and 4.3) (Zhi & Ying, 1993). These reactions represent the dissolution reaction in the experiments.

$$Mg_2SiO_4 + 2H_3O^+ \rightarrow 2Mg^{2+} + H_4SiO_4 + 2H_2O \quad (4.2)$$

$$NaAlSi_3O_8 + H_3O^+ \rightarrow Na^+ + HAlSi_3O_8 + H_2O \quad (4.3)$$

The pH values in the biotic flasks were slightly lower than in the abiotic sets. There were two other acidification sources in the experimental system other than sulfuric acid addition. Lysates of the bacterial cells result in a slight decrease in the pH (Gunes & Balci, 2021). Secondly, iron hydroxide formations by the hydrolysis of Fe(III) cause the proton release to water (Reactions 4.4-6) (Daoud & Karamanev, 2006). However, these acidification sources were not enough to keep the pH lower than 3.0.

$$Fe^{3+} + H_2O \leftrightarrow FeOH^{2+} + H^+ \quad (4.4)$$

$$Fe^{3+} + 2H_2O \leftrightarrow Fe(OH)_2^+ + H^+ \quad (4.5)$$

$$Fe^{3+} + 3H_2O \leftrightarrow Fe(OH)_3 + H^+ \quad (4.6)$$

### 4.3 Biosignature Potential of Microbially Mediated Basalt Dissolution Under Acidic Conditions

Biosignature identification has been a subject of great interest not only for understanding how life started on early Earth but also for searching for life on other planets such as Mars.

Biosignatures are the materials and structures whose origin indicates and requires the presence and effect of organisms (Hays et al., 2017). Organic molecules, especially biomolecules, are one of the most accurate biosignatures, and they are the best targets to trace the sign of life (Cabrol, 2018). However, organic molecules are degraded over time by environmental conditions. For example, Martian surface conditions are harsh for organic molecules to be preserved. Martian radiation and oxidants in the soil cause the degradation of organic molecules (Parnell et al., 2007). Furthermore, high amounts of hydrogen peroxide identified in Martian soil with the Viking mission is a strong oxidizer to change the structures of organic molecules (Piera & Bäckvall, 2008). Therefore, organic molecules are not considered as reliable biosignatures to search for ancient and possible present life on Mars. Mineralogical and geochemical biosignatures are the products of microbe-mineral interactions that are thought to be preserved on Mars (Banfield et al., 2001).

Mafic and ultramafic rocks occupy wide places on the Martian surface, and basalts are one of the most abundant rocks (Bibring et al., 2005). Acidic condition-related chemical weathering is one of the mechanisms that has been proposed for Martian geological history (Hurowitz & McLennan, 2007; Ehlmann et al., 2016). Mössbauer spectrometer on the Opportunity Rover detected the Fe-sulfate mineral, jarosite formations within the olivine- and pyroxene-bearing materials in the Meridiani Planum at Eagle Crater (Christensen et al., 2004; Klingelhöfer et al., 2004). Thus, understanding key microbial processes occurring on ultramafic and mafic rocks may help extend our understanding search for a sign of life beyond our solar system.

In the presented thesis, acid dissolution of basaltic rocks is of particular interest to reveal possible biological signatures during the acidic microbial dissolution of basalts and my motivation comes from Fe-bearing phases identified at the Meridiani Planum on Mars. The Fe-sulfate bearing phases-jarosite identified by remote sensing studies is attributed to acidic and oxidizing aqueous environments. Under acidic conditions,

the formation of ferric hydroxysulfate such as jarosite is generally attributed to the biological activity of chemolithotrophic bacteria such as *A. ferrooxidans*. *A. ferrooxidans* catalyzes Fe(II) oxidation to Fe(III) otherwise kinetically and thermodynamically extremely slow. As a result, the produced Fe(III) hydrolyze to form hydroxysulfates minerals with the formula $MFe_3(SO_4)_2(OH)_6$ where M = $K^+$, $Na^+$, $NH_4^+$, $Ag^+$, or $H_3O^+$ is produced (Daoud & Karamanev, 2006).

Jarosite and gypsum identified only in biotic experiments, BS1-B and BS2-B, suggest the influence of microbial reactions for their formations as explained above. Consistent with the results of this study, different laboratory-based experiments demonstrated jarosite formation by *A. ferrooxidans* by using different ferrous iron sources (Grishin et al., 1988; Daoud & Karamanev, 2006; Dopson et al., 2009; Wang et al., 2013). In addition, field-based studies showed that the presence of jarosite and other Fe-sulfate mineral schwertmannite formations related to *A. ferrooxidans* metabolism in the AMD sites (Egal et al., 2009; Wang & Zhou, 2012; Balci & Demirel, 2018; Bao et al., 2018). Additionally, different iron-oxide species were observed by microbial oxidation of iron (Napieralski et al., 2019; Yang et al., 2020).

In the presented thesis, although sulfate was present under all experimental conditions identification of jarosite and gypsum only in the biological experiments are suggestive of their microbially mediated formations. However, constraining kinetics and thermodynamic conditions favoring jarosite formation and stability are needed to make a robust conclusion. Nevertheless, the mineralogical and geochemical composition of Mars surface and subsurface vastly covered by basaltic rocks could have been favorable for chemolithoautotrophic metabolism (Boston et al., 1992) and macro/micronutrients may have been available once for life (Bibring et al., 2007; Treiman et al., 2016). If so, sulfate-bearing Fe oxides such as those identified in this study may be a good target for looking for biosignatures.

## 5. CONCLUSION

- The MPN results along with elemental concentrations, especially Fe, showed that the dissolution of the basalt rocks under acidic conditions create a suitable environment for the survival and growth of *Acidithiobacillus ferrooxidans* bacteria.
- Mineralogical identification of the pre and post reacted basalt grains revealed no mineralogical differences among the abiotic samples but Fe-bearing phases were identified under biotic conditions. SEM and elemental mappings of the surface of the post-reacted basalt grains showing Fe enrichment are further consistent with these results.
- Although sulfate was present in all experimental conditions, the formation of Fe bearing-sulfate mineral jarosite was only identified in the biotic experiments. This suggests that microbially induced jarosite formation is facilitated by Fe(II) oxidation rate under acidic conditions.
- The calculated $SiO_{2(aq)}$, Ca, and Mg release rates did not show significant differences between biotic and abiotic experiments. Lack of the cell size pits on the surface of the post reacted basalt rocks suggest that *A. ferrooxidans* did not attach to the surface of the rocks, implying that reactive fluid–rock interaction regulated the main dissolution reaction.
- This study showed that bacterial activity resulted in jarosite and gypsum formation during the dissolution of basaltic grains under acidic conditions and suggest that Fe sulfate bearing phases may have the potential to carry traces of biological activity that may be used as biosignatures here on Earth and Mars.

## 6. ACKNOWLEDGEMENTS

This M.Sc. thesis was supported by Istanbul Technical University Research Division (ITU-BAP) (Project Number: 42411) and TUBITAK (The Scientific and Technological Research Council of Turkey) grant to Nurgül BALCI (Project Number: 119Y411). I would like to thank Prof. Ali Haydar Gültekin and Dr. Alp Ünal for providing the basalt samples.

## 7. REFERENCES


**Akcil, A., & Koldas, S.** (2006). Acid Mine Drainage (AMD): causes, treatment and case studies. *Journal of Cleaner Production*, *14*(12-13 SPEC. ISS.), 1139–1145. https://doi.org/10.1016/j.jclepro.2004.09.006

**Andrews-Hanna, J. C., Phillips, R. J., & Zuber, M. T.** (2007). Meridiani Planum and the global hydrology of Mars. *Nature*, *446*(7132), 163–166. https://doi.org/10.1038/nature05594

**Aytar, P., Kay, C. M., Mutlu, M. B., Çabuk, A., & Johnson, D. B.** (2015). Diversity of acidophilic prokaryotes at two acid mine drainage sites in Turkey. *Environmental Science and Pollution Research*, *22*(8), 5995–6003. https://doi.org/10.1007/s11356-014-3789-4

**Baker, B. J., & Banfield, J. F.** (2003). Microbial communities in acid mine drainage. *FEMS Microbiology Ecology*, *44*(2), 139–152. https://doi.org/10.1016/S0168-6496(03)00028-X

**Balci, N., Shanks III, W. C., Mayer, B., & Mandernack, K. W.** (2007). Oxygen and sulfur isotope systematics of sulfate produced by bacterial and abiotic oxidation of pyrite. *Geochimica et Cosmochimica Acta 71*(15), 3796-3811. https://doi.org/10.1016/j.gca.2007.04.017

**Balci, N., Mayer, B., Shanks III, W. C., & Mandernack, K. W.** (2012). Oxygen and sulfur isotope systematics of sulfate produced during abiotic and bacterial oxidation of sphalerite and elemental sulfur. *Geochimica et Cosmochimica Acta 77*, 335-351. https://doi.org/10.1016/j.gca.2011.10.022.

**Balci, N., & Demirel, C.** (2016). Formation of carbonate nanoglobules by a mixed natural culture under hypersaline conditions. *Minerals*, *6*(4). https://doi.org/10.3390/min6040122

**Balci, N., & Demirel, C.** (2018). Prediction of acid mine drainage (AMD) and metal release sources at the Küre Copper Mine Site, Kastamonu, NW Turkey. *Mine Water and the Environment*, *37*(1), 56–74. https://doi.org/10.1007/s10230-017-0470-4

**Banerjee, N. R., Izawa, M. R. M., Sapers, H. M., & Whitehouse, M. J.** (2011). Geochemical biosignatures preserved in microbially altered basaltic glass. *Surface and Interface Analysis*, *43*(1–2), 452–457. https://doi.org/10.1002/sia.3577

**Banfield, Jillian F.; Moreau, John W.; Chan, Clara S.; Welch, Susan A.; Little, B.** (2001). Mineralogical Biosignatures and the Search for Life on Mars. *Astrobiology*, *1*(4), 447–465. https://doi.org/10.1016/b978-0-12-799965-4.00003-0

**Bao, Y., Guo, C., Lu, G., Yi, X., Wang, H., & Dang, Z.** (2018). Role of microbial activity in Fe(III) hydroxysulfate mineral transformations in an acid mine drainage-impacted site from the Dabaoshan Mine. *Science of the Total Environment*, *616–617*, 647–657. https://doi.org/10.1016/j.scitotenv.2017.10.273

**Barker, W. W., Welch, S. A., & Banfield, J. F.** (2019). Biogeochemical weathering of silicate minerals. *Geomicrobiology: Interactions Between Microbes and Minerals*, (Balkwill 1989), 391–428. https://doi.org/10.1515/9781501509247

**Bauermeister, A., Rettberg, P., & Flemming, H. C.** (2013). Growth of the acidophilic iron-sulfur bacterium Acidithiobacillus ferrooxidans under Mars-like geochemical conditions. *Planetary and Space Science*, *98*, 205–215. https://doi.org/10.1016/j.pss.2013.09.009

**Bibring, J.-P., Arvidson, R. E., Gendrin, A., Gondet, B., Langevin, Y., Le Mouelic, S., … Sotin, C.** (2007). Coupled Ferric Oxides and Sulfates on the Martian Surface. *Science*, *317*(5842), 1206–1210. https://doi.org/10.1126/science.1144174

**Bibring, J. P., Langevin, Y., Gendrin, A., Gondet, B., Poulet, F., Berthé, M., … Forget, F.** (2005). Mars surface diversity as revealed by the OMEGA/Mars express observations. *Science*, *307*(5715), 1576–1581. https://doi.org/10.1126/science.1108806

**Bibring, J. P., Langevin, Y., Mustard, J. F., Poulet, F., Arvidson, R., Gendrin, A., … Neukum, G.** (2006). Global mineralogical and aqueous Mars history derived from OMEGA/Mars express data. *Science*, *312*(5772), 400–404. https://doi.org/10.1126/science.1122659

**Bigham, J. M. & Nordstrom, D. K.** (2000). Iron and aluminum hydroxysulfates from acid sulfate waters. *Reviews in Mineralogy and Geochemistry 40*(1): 351-403, https://doi.org/ 10.2138/rmg.2000.40.7

**Bishop, J. L., Noe Dobrea, E. Z., McKeown, N. K., Parente, M., Ehlmann, B. L., Michalski, J. R., … Bibring, J.-P.** (2008). Phyllosilicate Diversity and Past Aqueous Activity Revealed at Mawrth Vallis, Mars. *Science*, *321*(5890), 830–833. https://doi.org/10.1126/science.1159699

**Boston, P. J., Ivanov, M. V., & McKay, C. P.** (1992). On the Possibility of Chemosynthetic Ecosystems in Subsurface Habitats on Mars. *Icarus*, *95*, 300–308. https://doi.org/10.1016/0019-1035(92)90045-9

**Brantley, S. L.** (2008). Kinetics of mineral dissolution. In: *Kinetics of Water-Rock Interaction*. (Eds. Brantley, S. L., Kubicki, J. D., and White, A. F.), Springer ScienceBusiness Media LLC, New York, NY, pp. 151-210.

**Brehm, U., Gorbushina, A., & Mottershead, D**. (2005). The role of microorganisms and biofilms in the breakdown and dissolution of quartz and glass. In *Geobiology: Objectives, Concepts, Perspectives*. https://doi.org/10.1016/B978-0-444-52019-7.50011-5

**Cabrol, N. A.** (2018). The Coevolution of Life and Environment on Mars: An Ecosystem Perspective on the Robotic Exploration of Biosignatures. *Astrobiology*, *18*(1), 1–27. https://doi.org/10.1089/ast.2017.1756

**Chandrapati, S., & Williams, M. G.** (2014). Total viable counts: Most probable number (MPN). In: *Encyclopedia of Food Microbiology* (2nd ed.). (Eds. Batt, C. A., & Tortorello, M. L.) Academic Press, pp. 621-624.

**Christensen, P. R., Wyatt, M. B., Glotch, T. D., Rogers, A. D., Anwar, S., Arvidson, R. E., … Wolff, M. J.** (2004). Mineralogy at Meridiani Planum from the Mini-TES experiment on the opportunity rover. *Science*, *306*(5702), 1733–1739. https://doi.org/10.1126/science.1104909

**Cockell, C. S., Bush, T., Bryce, C., Direito, S., Fox-Powell, M., Harrison, J. P., … Zorzano, M. P.** (2016). Habitability: A Review. *Astrobiology*, *16*(1), 89–117. https://doi.org/10.1089/ast.2015.1295

**Cockell, Charles S.** (2014). Trajectories of martian habitability. *Astrobiology*, *14*(2), 182–203. https://doi.org/10.1089/ast.2013.1106

**Cornell, R. M., Giovanoli, R., & Schneider, W.** (1989). Review of the hydrolysis of iron(III) and the crystallization of amorphous iron(III) hydroxide hydrate. *Journal of Chemical Technology & Biotechnology*, *46*(2), 115–134. https://doi.org/10.1002/jctb.280460204

**Daoud, J., & Karamanev, D.** (2006). Formation of jarosite during Fe2+ oxidation by Acidithiobacillus ferrooxidans. *Minerals Engineering*, *19*(9), 960–967. https://doi.org/10.1016/j.mineng.2005.10.024

**Dartnell, L. R., Desorgher, L., Ward, J. M., & Coates, A. J.** (2007). Modelling the surface and subsurface Martian radiation environment: Implications for astrobiology. *Geophysical Research Letters*, *34*(2), 4–9. https://doi.org/10.1029/2006GL027494

**Daye, M., Klepac-Ceraj, V., Pajusalu, M., Rowland, S., Farrell-Sherman, A., Beukes, N., … Bosak, T.** (2019). Light-driven anaerobic microbial oxidation of manganese. *Nature*, *576*(7786), 311–314. https://doi.org/10.1038/s41586-019-1804-0

**Dessert, C., Dupré, B., Gaillardet, J., François, L. M., & Allègre, C. J.** (2003). Basalt weathering laws and the impact of basalt weathering on the global carbon cycle. *Chemical Geology*, *202*(3–4), 257–273. https://doi.org/10.1016/j.chemgeo.2002.10.001

**Dopson, M., Lövgren, L., & Boström, D.** (2009). Silicate mineral dissolution in the presence of acidophilic microorganisms: Implications for heap bioleaching. *Hydrometallurgy*, *96*(4), 288–293. https://doi.org/10.1016/j.hydromet.2008.11.004

**Drever, J. I., & Stillings, L. L.** (1997). The role of organic acids in mineral weathering. *Colloids and Surfaces A: Physicochemical and Engineering Aspects*, *120*, 167–181.

**Egal, M., Casiot, C., Morin, G., Parmentier, M., Bruneel, O., Lebrun, S., & Elbaz-Poulichet, F.** (2009). Kinetic control on the formation of tooeleite, schwertmannite and jarosite by Acidithiobacillus ferrooxidans strains in an As(III)-rich acid mine water. *Chemical Geology*, *265*(3–4), 432–441. https://doi.org/10.1016/j.chemgeo.2009.05.008

**Ehlmann, B. L., Mustard, J. F., Fassett, C. I., Schon, S. C., Head, J. W., Des Marais, D. J., … Murchie, S. L.** (2008). Clay minerals in delta deposits and organic preservation potential on Mars. *Nature Geoscience*, *1*(6), 355–358. https://doi.org/10.1038/ngeo207

**Ehlmann, B. L., Mustard, J. F., Swayze, G. A., Clark, R. N., Bishop, J. L., Poulet, F., … Murchie, S. L.** (2009). Identification of hydrated silicate minerals on Mars using MRO-CRISM: Geologic context near Nili Fossae and implications for aqueous alteration. *Journal of Geophysical Research E: Planets*, *114*(10), 1–33. https://doi.org/10.1029/2009JE003339

**Ehlmann, B. L., Swayze, G. A., Milliken, R. E., Mustard, J. F., Clark, R. N., Murchie, S. L., … Seelos, K. D.** (2016). Discovery of alunite in cross crater, terra sirenum, mars: Evidence for acidic, sulfurous waters. *American Mineralogist*, *101*(7), 1527–1542. https://doi.org/10.2138/am-2016-5574

**Fairén, A. G., Davilla, A. F., Lim, D., Bramall, N., Bonaccorsi, R., Zavaleta, J., Uceda, E. R., Stoker, C., Wierzchos, J., Dohm, J. M., Amils, R., Andersen, D., & McKay, C. P.,** (2010) Astrobiology through the ages of Mas: The study of terrestrial analogues to understand the habitability of Mars. *Astrobiology 10*(8), 821-843, https://doi.org/10.1089/ast.2009.0440

**Gale, N. L., & Beck, J. V.** (1967). Evidence for the Calvin cycle and hexose monophosphate pathway in Thiobacillus ferrooxidans. *Journal of Bacteriology*, *94*(4), 1052–1059. https://doi.org/10.1128/jb.94.4.1052-1059.1967

**Garcia, B., Lemelle, L., Rose-Koga, E., Perriat, P., Basset, R., Gillet, P., & Albarède, F.** (2013). An experimental model approach of biologically-assisted silicate dissolution with olivine and Escherichia coli - Impact on chemical weathering of mafic rocks and atmospheric CO2 drawdown. *Applied Geochemistry*, *31*(November), 216–227. https://doi.org/10.1016/j.apgeochem.2013.01.007

**González-Toril, E., Llobet-Brossa, E., Casamayor, E. O., Amann, R., & Amils, R**. (2003). Microbial ecology of an extreme acidic environment, the Tinto River. *Applied and Environmental Microbiology*, *69*(8), 4853–4865. https://doi.org/10.1128/AEM.69.8.4853-4865.2003

**Grishin, S. I., Bigham, J. M., & Tuovinen, O. H.** (1988). Characterization of Jarosite Formed upon Bacterial Oxidation of Ferrous Sulfate. *Applied and Environmental Microbiology*, *54*(12), 3101–3106.

**Gudbrandsson, S., Wolff-Boenisch, D., Gislason, S. R., & Oelkers, E. H.** (2011). An experimental study of crystalline basalt dissolution from 2pH11 and temperatures from 5 to 75°C. *Geochimica et Cosmochimica Acta*, *75*(19), 5496–5509. https://doi.org/10.1016/j.gca.2011.06.035

**Gunes, Y., & Balci, N.** (2021). The Catalytic Effect of the Heterotrophic Bacterium Virgibacillus marismortui on Basaltic Rock Dissolution Under Excess Nutrient Conditions. *Geomicrobiology Journal*, *38*:4, 315-328. https://doi.org/10.1080/01490451.2020.1852453

**Hartmann, J., West, A. J., Renforth, P., Köhler, P., De La Rocha, C. L., Wolf-Gladrow, D. A., … Scheffran, J.** (2013). Enhanced chemical weathering as a geoengineering strategy to reduce atmospheric carbon dioxide, supply nutrients, and mitigate ocean acidification. *Reviews of Geophysics*, *51*(2), 113–149. https://doi.org/10.1002/rog.20004

**Hausrath, E. M., Neaman, A., & Brantley, S. L.** (2009). Elemental release rates from dissolving basalt and granite with and without organic ligands. *American Journal of Science*, *309*(8), 633–660. https://doi.org/10.2475/08.2009.01

**Hays, L. E., Graham, H. V., Des Marais, D. J., Hausrath, E. M., Horgan, B., McCollom, T. M., … Lynch, K. L.** (2017). Biosignature Preservation and Detection in Mars Analog Environments. *Astrobiology*, *17*(4), 363–400. https://doi.org/10.1089/ast.2016.1627

**Head, J. W., Neukum, G., Jaumann, R., Hiesinger, H., Hauber, E., Carr, M., … Van Gasselt, S.** (2005). Tropical to mid-latitude snow and ice accumulation, flow and glaciation on Mars. *Nature*, *434*(7031), 346–351. https://doi.org/10.1038/nature03359

**Hellmann, R. Wirth, R., Daval, D., Barnes, J. P., Penisson, J. M., Tisserand, D., Epicier, T., Florin, B. & Hervig, R. L.** (2012). Unifying natural and laboratory chemical weathering with interficial dissolution-reprecipitation: A study based on the nanometer-scale chemistry of fluid-silicate interfaces. *Chemical Geology 294-295:* 203-216. https://doi.org/10.1016/j.chemgeo.2011.12.002

**Horgan, B. H. N., Smith, R. J., Cloutis, E. A., Mann, P., & Christensen, P. R.** (2017). Acidic weathering of basalt and basaltic glass: 1. Near-infrared spectra, thermal infrared spectra, and implications for Mars. *Journal of Geophysical Research: Planets*, *122*(1), 172–202. https://doi.org/10.1002/2016JE005111

**Huang, L. N., Kuang, J. L., & Shu, W. S.** (2016). Microbial Ecology and Evolution in the Acid Mine Drainage Model System. *Trends in Microbiology*, *24*(7), 581–593. https://doi.org/10.1016/j.tim.2016.03.004

**Hurowitz, J. A., Fischer, W. W., Tosca, N. J., & Milliken, R. E.** (2010). Origin of acidic surface waters and the evolutionof atmospheric chemistry on early Mars. *Nature Geoscience*, *3*(5), 323–326. https://doi.org/10.1038/ngeo831

**Hurowitz, J. A., & McLennan, S. M.** (2007). A ∼ 3.5 Ga record of water-limited, acidic weathering conditions on Mars. *Earth and Planetary Science Letters*, *260*(3–4), 432–443. https://doi.org/10.1016/j.epsl.2007.05.043

**King, P. L., & McLennan, S. M.** (2010). Sulfur on mars. *Elements*, *6*(2), 107–112. https://doi.org/10.2113/gselements.6.2.107

**Klingelhöfer, G., Morris, R. V, Bernhardt, B., Schröder, C., Radionov, D. S., de Souza Jr., P. A., … Arvidson, R. E.** (2004). Jarosite and Hematite at Meridiani Planum from Opportunity's Mössbauer Spectrometer. *Science*, *306*(5702), 1740–1745. https://doi.org/10.1126/science.1104653

**Knowles, E., Staudigel, H., & Templeton, A.** (2013). Geochemical characterization of tubular alteration features in subseafloor basalt glass. *Earth and Planetary Science Letters*, *374*, 239–250. https://doi.org/10.1016/j.epsl.2013.05.012

**Kuypers, M. M. M., Marchant, H. K., & Kartal, B.** (2018). The microbial nitrogen-cycling network. *Nature Reviews Microbiology*, *16*(5), 263–276. https://doi.org/10.1038/nrmicro.2018.9

**Lamérand, C., Shirokova, L. S., Bénézeth, P., Rols, J. L., & Pokrovsky, O. S.** (2020). Olivine dissolution and hydrous Mg carbonate and silicate precipitation in the presence of microbial consortium of photo-autotrophic and heterotrophic bacteria. *Geochimica et Cosmochimica Acta*, *268*, 123–141. https://doi.org/10.1016/j.gca.2019.09.040

**Léveillé, R. J., Longstaffe, F. J., & Fyfe, W. S.** (2007). An isotopic and geochemical study of carbonate-clay mineralization in basaltic caves: Abiotic versus microbial processes. *Geobiology*, *5*(3), 235–249. https://doi.org/10.1111/j.1472-4669.2007.00109.x

**Mackintosh, M. E.** (1978). Nitrogen fixation by Thiobacillus ferrooxidans. *Journal of General Microbiology*, *105*(2), 215–218. https://doi.org/10.1099/00221287-105-2-215

**Madden, M. E. E., Bodnar, R. J., & Rimstidt, J. D.** (2004). Jarosite as an indicator of water-limited chemical weathering on Mars. *Nature*, *431*(7010), 821–823. https://doi.org/10.1038/nature02971

**Mangold, N., Schmidt, M. E., Fisk, M. R., Forni, O., McLennan, S. M., Ming, D. W., … Wiens, R. C.** (2017). Classification scheme for sedimentary and igneous rocks in Gale crater, Mars. *Icarus*, *284*, 1–17. https://doi.org/10.1016/j.icarus.2016.11.005

**McCollom, T. M., Robbins, M., Moskowitz, B., Berquõ, T. S., Jöns, N., & Hynek, B. M.** (2013). Experimental study of acid-sulfate alteration of basalt and implications for sulfate deposits on Mars. *Journal of Geophysical Research E: Planets*, *118*(4), 577–614. https://doi.org/10.1002/jgre.20044

**McKay, C. P., & Marinova, M. M.** (2001). The physics, biology, and environmental ethics of making mars habitable. *Astrobiology*, *1*(1), 89–109. https://doi.org/10.1089/153110701750137477

**McKinley, J. P., Stevens, T. O., & Westall, F.** (2000). Microfossils and paleoenvironments in deep subsurface basalt samples. *Geomicrobiology Journal*, *17*(1), 43–54. https://doi.org/10.1080/014904500270486

**Méndez-García, C., Peláez, A. I., Mesa, V., Sánchez, J., Golyshina, O. V., & Ferrer, M.** (2015). Microbial diversity and metabolic networks in acid mine drainage habitats. *Frontiers in Microbiology*, *6*(MAY), 1–17. https://doi.org/10.3389/fmicb.2015.00475

**Morgan, B., & Lahav, O.** (2007). The effect of pH on the kinetics of spontaneous Fe(II) oxidation by O2 in aqueous solution - basic principles and a simple heuristic description. *Chemosphere*, *68*(11), 2080–2084. https://doi.org/10.1016/j.chemosphere.2007.02.015

**Napieralski, S. A., Buss, H. L., Brantley, S. L., Lee, S., Xu, H., & Roden, E. E.** (2019). Microbial chemolithotrophy mediates oxidative weathering of granitic bedrock. *Proceedings of the National Academy of Sciences of the United States of America*, *116*(52), 26394–26401. https://doi.org/10.1073/pnas.1909970117

**Navarrete, J. U., Cappelle, I. J., Schnittker, K., & Borrok, D. M.** (2013). Bioleaching of ilmenite and basalt in the presence of iron-oxidizing and iron-scavenging bacteria. *International Journal of Astrobiology*, *12*(2), 123–134. https://doi.org/10.1017/s1473550412000493

**Navrotsky, A., Forray, F. L., & Drouet, C.** (2005). Jarosite stability on Mars. *Icarus*, *176*(1), 250–253. https://doi.org/10.1016/j.icarus.2005.02.003

**Norlund, K. L. I., Southam, G., Tyliszczak, T., Hu, Y., Karunakaran, C., Obst, M., … Warren, L. A.** (2009). Microbial architecture of environmental sulfur processes: A novel syntrophic sulfur-metabolizing consortia. *Environmental Science and Technology*, *43*(23), 8781–8786. https://doi.org/10.1021/es803616k

**Olsson-francis, K., Pearson, V. K., Steer, E. D., & Schwenzer, S. P.** (2017). Determination of Geochemical Bio-Signatures in Mars-Like Basaltic Environments. *Frontiers in Microbiology*, *8*(September). https://doi.org/10.3389/fmicb.2017.01668

**Olsson-Francis, K., Simpson, A. E., Wolff-Boenisch, D., & Cockell, C. S.** (2012). The effect of rock composition on cyanobacterial weathering of crystalline basalt and rhyolite. *Geobiology*, *10*(5), 434–444. https://doi.org/10.1111/j.1472-4669.2012.00333.x

**Parnell, J., Cullen, D., Sims, M. R., Bowden, S., Cockell, C. S., Court, R., … Vago, J.** (2007). Searching for life on Mars: Selection of molecular targets for ESA's Aurora ExoMars mission. *Astrobiology*, *7*(4), 578–604. https://doi.org/10.1089/ast.2006.0110

**Peretyazhko, T. S., Niles, P. B., Sutter, B., Morris, R. V., Agresti, D. G., Le, L., & Ming, D. W.** (2018). Smectite formation in the presence of sulfuric acid: Implications for acidic smectite formation on early Mars. *Geochimica et Cosmochimica Acta*, *220*, 248–260. https://doi.org/10.1016/j.gca.2017.10.004

**Perez, A., Rossano, S., Trcera, N., Huguenot, D., Fourdrin, C., Verney-Carron, A., … Guyot, F.** (2016). Bioalteration of synthetic Fe(III)-, Fe(II)-bearing basaltic glasses and Fe-free glass in the presence of the heterotrophic bacteria strain Pseudomonas aeruginosa: Impact of siderophores. *Geochimica et Cosmochimica Acta*, *188*, 147–162. https://doi.org/10.1016/j.gca.2016.05.028

**Piera, J., & Bäckvall, J. E.** (2008). Catalytic oxidation of organic substrates by molecular oxygen and hydrogen peroxide by multistep electron transfer - A biomimetic approach. *Angewandte Chemie - International Edition*, *47*(19), 3506–3523. https://doi.org/10.1002/anie.200700604

**Preston, L. J., Izawa, M. R. M., & Banerjee, N. R.** (2011). Infrared spectroscopic characterization of organic matter associated with microbial bioalteration textures in basaltic glass. *Astrobiology*, *11*(7), 585–599. https://doi.org/10.1089/ast.2010.0604

**Ruiz-Agudo, E., Putnis, C. V., & Putnis, A.** (2014). Coupled dissolution and precipitation at mineral-fluid interfaces. *Chemical Geology 383*, 132-146, https://doi.org/10.1016/j.chemgeo.2014.06.007

**Sağlam, E. S., Akçay, M., Çolak, D. N., İnan Bektaş, K., & Beldüz, A. O.** (2016). Generation of acid mine drainage around the Karaerik copper mine (Espiye, Giresun, NE Turkey): implications from the bacterial population in the Acısu effluent. *Extremophiles*, *20*(5), 673–685. https://doi.org/10.1007/s00792-016-0857-3

**Sand, W.** (1989). Ferric iron reduction by Thiobacillus ferrooxidans at extremely low pH-values. *Biogeochemistry*, *7*(3), 195–201. https://doi.org/10.1007/BF00004217

**Sand, W., & Gehrke, T.** (2006). Extracellular polymeric substances mediate bioleaching/biocorrosion via interfacial processes involving iron(III) ions and acidophilic bacteria. *Research in Microbiology*, *157*(1), 49–56. https://doi.org/10.1016/j.resmic.2005.07.012

**Santelli, C. M., Welch, S. A., Westrich, H. R., & Banfield, J. F.** (2001). The effect of Fe-oxidizing bacteria on Fe-silicate mineral dissolution. *Chemical Geology*, *180*(1–4), 99–115. https://doi.org/10.1016/S0009-2541(01)00308-4

**Schott, J., Pokrovsky, O. S., & Oelkers, E. H.** (2009). The link between mineral dissolution/precipitation kinetics and solution chemistry. In: *Thermodynamics and Kinetics of Water-Rock Interaction*. (Eds. Oelkers, E. H. & Schott, J.), pp.207-258.

**Schrenk, M., J. Edwards, K., M. Goodman, R., J. Hamers, R., & F. Banfield, J.** (1998). Distribution of Thiobacillus ferrooxidans and Leptospirillum ferrooxidans: implications for generation of acid mine drainage. *Science*, Vol. 279, pp. 1519–1521. https://doi.org/10.1126/science.279.5356.1519

**Schwartzman, D. W., & Volk, T.** (1989). Biotic enhancement of weathering and the habitability of Earth. *Nature*, *340*(6233), 457–460. https://doi.org/10.1038/340457a0

**Smith, P. H., Tamppari, L. K., Arvidson, R. E., Bass, D., Blaney, D., Boynton, W. V, … Zent, A. P.** (2009). H2O at the Phoenix Landing Site. *Science*, *325*(5936), 58–61. https://doi.org/10.1126/science.1172339

**Squyres, S. W., Arvidson, R. E., Bell, J. F., Calef, F., Clark, B. C., Cohen, B. A., … Zacny, K.** (2012). Ancient impact and aqueous processes at endeavour crater, Mars. *Science*, *336*(6081), 570–576. https://doi.org/10.1126/science.1220476

**Stockmann, G. J., Shirokova, L. S., Pokrovsky, O. S., Bénézeth, P., Bovet, N., Gislason, S. R., & Oelkers, E. H.** (2012). Does the presence of heterotrophic bacterium Pseudomonas reactans affect basaltic glass dissolution rates? *Chemical Geology*, *296–297*, 1–18. https://doi.org/10.1016/j.chemgeo.2011.12.011

**Teske, A. P.** (2005). The deep subsurface biosphere is alive and well. *Trends in Microbiology*, *13*(9), 402–404. https://doi.org/10.1016/j.tim.2005.07.004

**Tosca, N. J., McLennan, S. M., Lindsley, D. H., & Schoonen, M. A. A.** (2004). Acid-sulfate weathering of synthetic Martian basalt: The acid fog model revisited. *Journal of Geophysical Research E: Planets*, *109*(5). https://doi.org/10.1029/2003JE002218

**Treiman, A. H., Bish, D. L., Vaniman, D. T., Chipera, S. J., Blake, D. F., Ming, D. W., … Yen, A. S.** (2016). Mineralogy, provenance, and diagenesis of a potassic basaltic sandstone on Mars: CheMin X-ray diffraction of the Windjana sample (Kimberley area, Gale Crater). *Journal of Geophysical Research: Planets*, *121*, 75–106. https://doi.org/10.1002/2015JE004932

**Türke, A., Ménez, B., & Bach, W.** (2018). Comparing biosignatures in aged basalt glass from North Pond, Mid-Atlantic Ridge and the Louisville Seamount Trail, off New Zealand. *PLoS ONE*, *13*(2), 1–17. https://doi.org/10.1371/journal.pone.0190053

**Uroz, S., Calvaruso, C., Turpault, M. P., & Frey-Klett, P.** (2009). Mineral weathering by bacteria: ecology, actors and mechanisms. *Trends in Microbiology*, *17*(8), 378–387. https://doi.org/10.1016/j.tim.2009.05.004

**Valdés, J., Pedroso, I., Quatrini, R., Dodson, R. J., Tettelin, H., Blake, R., … Holmes, D. S.** (2008). Acidithiobacillus ferrooxidans metabolism: From genome sequence to industrial applications. *BMC Genomics*, *9*, 1–24. https://doi.org/10.1186/1471-2164-9-597

**Valdés, J., Veloso, F., Jedlicki, E., & Holmes, D.** (2003). Metabolic reconstruction of sulfur assimilation in the extremophile Acidithiobacillus ferrooxidans based on genome analysis. *BMC Genomics*, *4*, 1–16. https://doi.org/10.1186/1471-2164-4-51

**Vandevivere, P., Welch, S. A., Ullman, W. J., & Kirchman, D. L.** (1994). Enhanced Dissolution of Silicate Minerals by Bacteria at Near-Neutral pH. *Microbial Ecology*, *27*, 241–251. https://doi.org/https://doi.org/10.1007/BF00182408

**Wang, M., & Zhou, L.** (2012). Simultaneous oxidation and precipitation of iron using jarosite immobilized Acidithiobacillus ferrooxidans and its relevance to acid mine drainage. *Hydrometallurgy*, *125–126*, 152–156. https://doi.org/10.1016/j.hydromet.2012.06.003

**Wang, Y., Li, H., & Li, D.** (2013). Biosynthesis of natrojarosite by immobilized iron-oxidizing bacteria. *International Journal of Mineral Processing*, *120*, 35–38. https://doi.org/10.1016/j.minpro.2013.02.006

**Welch, S. A., & Ullman, W. J.** (1996). Feldspar dissolution in acidic and organic solutions: Compositional and pH dependence of dissolution rate. *Geochimica et Cosmochimica Acta*, *60*(16), 2939–2948. https://doi.org/10.1016/0016-7037(96)00134-2

**Welch, S. A., & Banfield, J. F**. (2002). Modification of olivine surface morphology and reactivity by microbial activity during chemical weathering. *Geochimica et Cosmochimica Acta*, *66*(2), 213–221. https://doi.org/10.1016/S0016-7037(01)00771-2

**Welch, S. A., & Ullman, W. J.** (1993). The effect of organic acids on plagioclase dissolution rates and stoichiometry. *Geochimica et Cosmochimica Acta*, *57*(12), 2725–2736. https://doi.org/10.1016/0016-7037(93)90386-B

**Wolff-Boenisch, D., Gislason, S. R., & Oelkers, E. H.** (2006). The effect of crystallinity on dissolution rates and CO2 consumption capacity of silicates. *Geochimica et Cosmochimica Acta*, *70*(4), 858–870. https://doi.org/10.1016/j.gca.2005.10.016

**Wu, L., Jacobson, A. D., Chen, H. C., & Hausner, M.** (2007). Characterization of elemental release during microbe-basalt interactions at T = 28 °C. *Geochimica et Cosmochimica Acta*, *71*(9), 2224–2239. https://doi.org/10.1016/j.gca.2007.02.017

**Yang, M., Zhan, Y., Zhang, S., Wang, W., & Yan, L.** (2020). Biological materials formed by Acidithiobacillus ferrooxidans and their potential applications. *3 Biotech*, *10*(11), 1–9. https://doi.org/10.1007/s13205-020-02463-3

**Zhan, Y., Yang, M., Zhang, S., Zhao, D., Duan, J., Wang, W., & Yan, L.** (2019). Iron and sulfur oxidation pathways of Acidithiobacillus ferrooxidans. *World Journal of Microbiology and Biotechnology*, *35*(4), 0. https://doi.org/10.1007/s11274-019-2632-y

**Zhi, D., & Ying, H.** (1993). A study on the dissolution kinetics of basalt-water interaction under different pH conditions I: Release of elements and pH neutralization effect. *Chinese Journal of Geochemistry*, *12*(2), 183–191. https://doi.org/10.1007/BF02842199

**Zolotov, M. Y., & Shock, E. L.** (2005). Formation of jarosite-bearing deposits through aqueous oxidation of pyrite at Meridiani Planum, Mars. *Geophysical Research Letters*, *32*(21), 1–5. https://doi.org/10.1029/2005GL024253

**APPENDIX A**

**Table A:** MPN Index values based on 95% confidence limits

| Number of tubes giving positive reaction out of | | | | Number of tubes giving positive reaction out of | | | |
|---|---|---|---|---|---|---|---|
| 5 undiluted samples (Dilution factor-1) | 5 dilutions of 10 (dilution factor-10) | 5 dilutions of 100 (dilution factor-100) | MPN Index per 100 ml | 5 undiluted samples (Dilution factor-1) | 5 dilutions of 10 (dilution factor-10) | 5 dilutions of 100 (dilution factor-100) | MPN Index per 100 ml |
| 0 | 0 | 0 | <1.8 | 3 | 3 | 0 | 17 |
| 0 | 0 | 1 | 1.8 | 3 | 3 | 1 | 21 |
| 0 | 1 | 0 | 1.8 | 3 | 3 | 2 | 24 |
| 0 | 1 | 1 | 3.6 | 3 | 4 | 0 | 21 |
| 0 | 2 | 0 | 3.7 | 3 | 4 | 1 | 24 |
| 0 | 2 | 1 | 5.5 | 3 | 5 | 0 | 25 |
| 0 | 3 | 0 | 5.6 | 4 | 0 | 0 | 13 |
| 1 | 0 | 0 | 2.0 | 4 | 0 | 1 | 17 |
| 1 | 0 | 1 | 4.0 | 4 | 0 | 2 | 21 |
| 1 | 0 | 2 | 6.0 | 4 | 0 | 3 | 25 |
| 1 | 1 | 0 | 4.0 | 4 | 1 | 0 | 17 |
| 1 | 1 | 1 | 6.1 | 4 | 1 | 1 | 21 |
| 1 | 1 | 2 | 8.1 | 4 | 1 | 2 | 26 |
| 1 | 2 | 0 | 6.1 | 4 | 1 | 3 | 31 |
| 1 | 2 | 1 | 8.2 | 4 | 2 | 0 | 22 |
| 1 | 3 | 0 | 8.3 | 4 | 2 | 1 | 26 |
| 1 | 3 | 1 | 10 | 4 | 2 | 2 | 32 |
| 1 | 4 | 0 | 11 | 4 | 2 | 3 | 38 |
| 2 | 0 | 0 | 4.5 | 4 | 3 | 0 | 27 |
| 2 | 0 | 1 | 6.8 | 4 | 3 | 1 | 33 |
| 2 | 0 | 2 | 9.1 | 4 | 3 | 2 | 39 |
| 2 | 1 | 0 | 6.8 | 4 | 4 | 0 | 34 |
| 2 | 1 | 1 | 9.2 | 4 | 4 | 1 | 40 |
| 2 | 1 | 2 | 12 | 4 | 4 | 2 | 47 |
| 2 | 2 | 0 | 9.3 | 4 | 5 | 0 | 41 |
| 2 | 2 | 1 | 12 | 4 | 5 | 1 | 48 |
| 2 | 2 | 2 | 14 | 5 | 0 | 0 | 23 |
| 2 | 3 | 0 | 12 | 5 | 0 | 1 | 31 |
| 2 | 3 | 1 | 14 | 5 | 0 | 2 | 43 |
| 2 | 4 | 0 | 15 | 5 | 0 | 3 | 58 |
| 3 | 0 | 0 | 7.8 | 5 | 1 | 0 | 33 |
| 3 | 0 | 1 | 11 | 5 | 1 | 1 | 46 |
| 3 | 0 | 2 | 13 | 5 | 1 | 2 | 63 |
| 3 | 1 | 0 | 11 | 5 | 1 | 3 | 84 |
| 3 | 1 | 1 | 14 | 5 | 2 | 0 | 49 |
| 3 | 1 | 2 | 17 | 5 | 2 | 1 | 70 |
| 3 | 2 | 0 | 14 | 5 | 2 | 2 | 94 |
| 3 | 2 | 1 | 17 | 5 | 2 | 3 | 120 |
| 3 | 2 | 2 | 20 | 5 | 2 | 4 | 150 |

**Table A (Continued):** MPN Index values based on 95% confidence limits

| Number of tubes giving positive reaction out of | | | | Number of tubes giving positive reaction out of | | | |
|---|---|---|---|---|---|---|---|
| 5 undiluted samples (Dilution factor-1) | 5 dilutions of 10 (dilution factor-10) | 5 dilutions of 100 (dilution factor-100) | MPN Index per 100 ml | 5 undiluted samples (Dilution factor-1) | 5 dilutions of 10 (dilution factor-10) | 5 dilutions of 100 (dilution factor-100) | MPN Index per 100 ml |
| 5 | 3 | 0 | 79 | 5 | 4 | 4 | 350 |
| 5 | 3 | 1 | 110 | 5 | 4 | 5 | 430 |
| 5 | 3 | 2 | 140 | 5 | 5 | 0 | 240 |
| 5 | 3 | 3 | 170 | 5 | 5 | 1 | 350 |
| 5 | 3 | 4 | 210 | 5 | 5 | 2 | 540 |
| 5 | 4 | 0 | 130 | 5 | 5 | 3 | 920 |
| 5 | 4 | 1 | 170 | 5 | 5 | 4 | 1600 |
| 5 | 4 | 2 | 220 | 5 | 5 | 5 | >1600 |
| 5 | 4 | 3 | 280 | | | | |

**CURRICULUM VITAE**

**Name Surname** **:** Fatih Şekerci

**EDUCATION:**

**B.Sc. :** 2018, Istanbul Technical University, Faculty of Science and Letters, Molecular Biology and Genetics Department

**M.Sc.:**2021, Istanbul Technical University, Graduate School, Geological Engineering Department

**PROFESSIONAL EXPERIENCE:**

- 2015-2017, General Secretary, Istanbul Technical University Molecular Biology and Genetics Student Club
- 2017, Summer Internship, Evolutionary Genetics Laboratory, Ankara University
- 2018-Present, Laboratory Member, Geomicrobiology and Biogeochemistry Laboratory, Istanbul Technical University
- 2018 ITU Rover Team, Science Team Member

**PUBLICATIONS, PRESENTATIONS AND PATENTS ON THE THESIS:**

- **Şekerci, F., Balcı, N., Gunes, Y., Gültekin, A.H.** 2020. Bazalt Bileşimli Kayaçların Ayrışmasında Mikrobiyal Etkiler ve Mars İçin Önermeleri, 9th Geochemistry Symposium, Aydin, Conference Paper. (accepted)
- **Şekerci, F.**, **Balcı, N., Güneş, Y., Gültekin, A.H.** 2020. Bazalt Bileşimli Kayaçların Ayrışmasında Mikrobiyal Etkiler ve Mars İçin Önermeleri, 73th Geological Congress of Turkey with International Participation, Poster Presentation.

**OTHER PUBLICATIONS, PRESENTATIONS AND PATENTS:**

- **Arisan, D., Şahin, Z., Erdoğdu, N. D., Şekerci, F., Doğanay, G. D., Kurt, M. A., Balcı, N.** 2019. Ne Kadar Kobalt Toksik? *Virgibacillus marismortui* Örneği, 72th Geological Congress of Turkey with International Participation, Oral Presentation.